Design and development of an autonomous guidance law by flatness approach

Application to an atmospheric reentry mission

by

Vincent MORIO

PhD Supervisor: Prof. Ali ZOLGHADRI

PhD Co-supervisor: Dr. Franck CAZAURANG

Automatic Control Group
IMS lab./Bordeaux University
France
http://extranet.ims-bordeaux.fr/aria

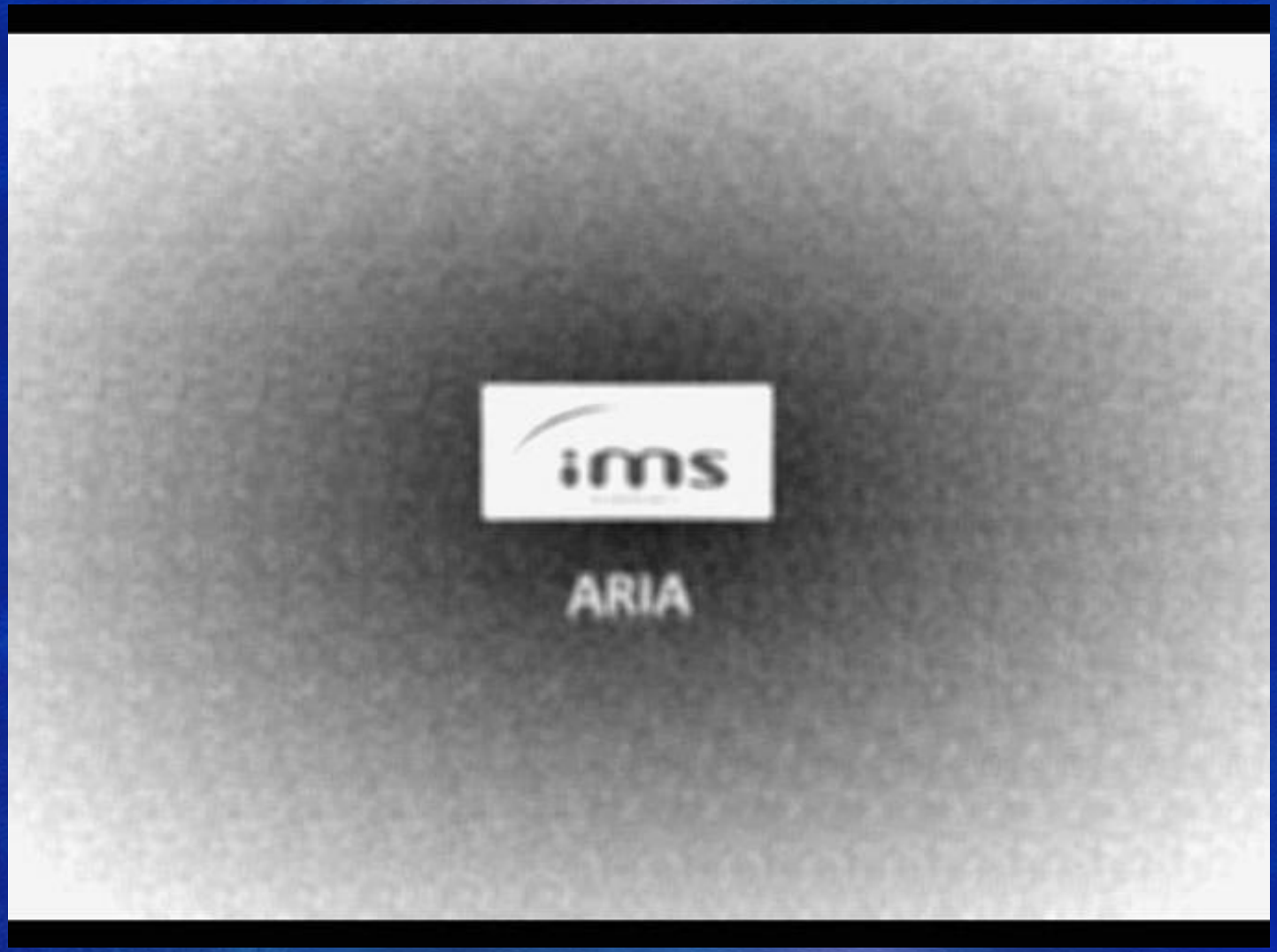

Atmospheric reentry guidance: TAEM and Autolanding phases

List of publications

Since october 2006:

- **4 international journal papers:**

[1] V. Morio, F. Cazaurang and P. Vernis, "Flatness-based Hypersonic Reentry Guidance of a Lifting-body Vehicle," **Control Engineering Practice**, 17(5):588-596, May 2009.

[2] V. Morio, F. Cazaurang, A. Zolghadri and P. Vernis, "Onboard Path Planning for Reusable Launch Vehicles. Application to the Shuttle Orbiter Reentry Mission," **International Review of Aerospace Engineering**, 1(6), December 2008.

[3] F. Cazaurang, V. Morio, A. Falcoz, D. Henry and A. Zolghadri, "New Model-Based Strategies for Guidance and Health Monitoring of Experimental Reentry Vehicles," **International Review of Aerospace Engineering**, 1(5):458-463, October 2008.

[4] V. Morio, F. Cazaurang, A. Falcoz and P. Vernis, "Robust Terminal Area Energy Management Guidance using Flatness Approach," **IET Control Theory and Applications**, 2009.

- **9 international conference papers:**

IEEE European Control Conference (ECC), IFAC World Congress, IFAC Symposium on Automatic Control in Aerospace (ACA), IEEE Multi-conference on Systems and Control (MSC), International ARA Days, Conférence Internationale Francophone d'Automatique (CIFA)

Outline

- Part I — Statement of the guidance problem
- Part II — Autonomous guidance law architecture
- Part III — Flatness-based trajectory planning
- Part IV — Fault-tolerant trajectory planning
- Part V — Integration of aerologic disturbances
- Part VI — Convexification methodology

Part I
Guidance problem statement: TAEM and A&L phases

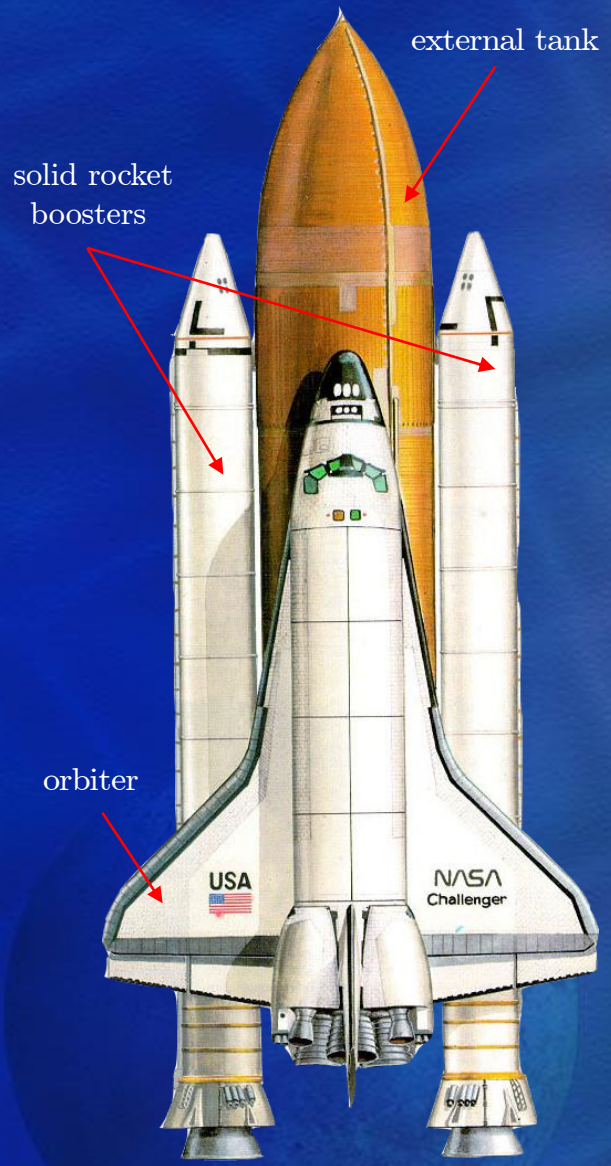

Space transportation system

- Mission:

  Insertion in low-Earth orbit of payloads and crews

- First flight: 04/12/1981,
- Total number of flights: 126 as of 05/11/2009,
- Mean cost per mission: from \$300M to \$400M (2006),
- 3 operational vehicles until 2010 (fleet retirement).

main features	**symbol**	**value**
reference area $[m^2]$	S	249.9
overall mass at injection point $[kg]$	m	89930
wingspan $[m]$	b	23.8
chord length $[m]$	$\bar{c}$	12
max. gliding ratio (for $M \leq 3$)	$(L/D)_{\max}$	≈ 4
inertial moments $[kg/m^2]$	I_{xx}	1213866
	I_{yy}	9378654
	I_{zz}	9759518
inertial products $[kg/m^2]$	I_{xz}	228209
	I_{xy}	6136
	I_{yz}	2972
moments reference center $[m]$	x_{mrc}	17
	y_{mrc}	0
	z_{mrc}	-1.2
center of gravity $[m]$	x_{cg}	27.3
	y_{cg}	0
	z_{cg}	9.5

Orbiter STS-1 main features

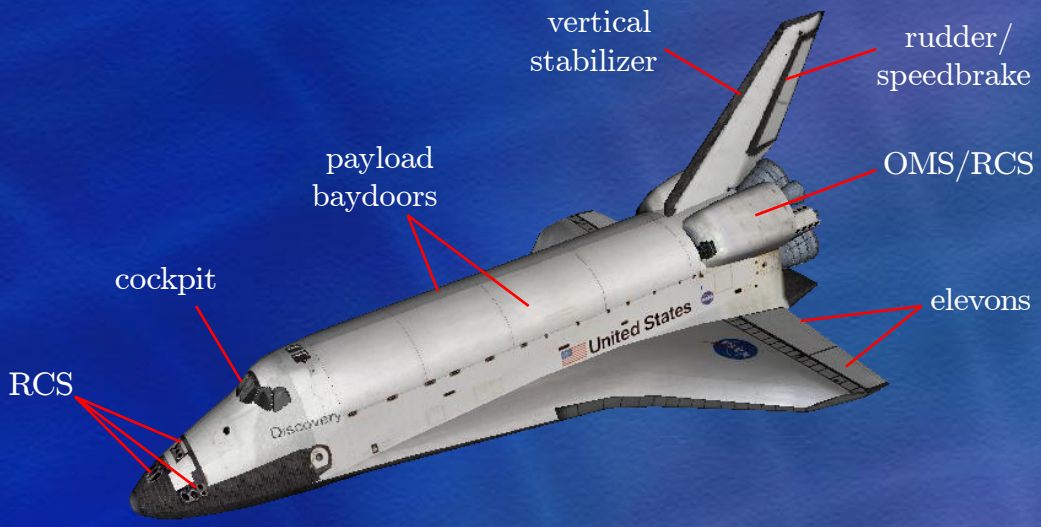

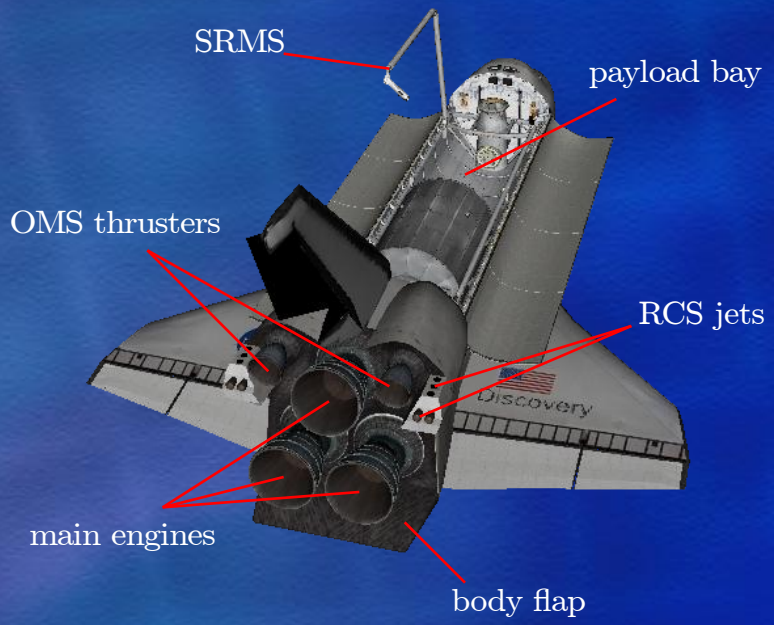

control surface	symbol	deflection limis min (deg)	deflection limis max (deg)	deflection rates (deg/s)
elevons				
pitching	δ_e	-35	20	20
ailerons	δ_a	-35	20	20
rudder	δ_r	-22.8	22.8	10
speedbrake	δ_{sb}	0	87.2	5
body flap	δ_{bf}	-11.7	22.55	1.3

control surfaces deflections limits and rates

3 main phases:

- Hypersonic entry
- Terminal Area Energy Management (TAEM)
- Autolanding phase (A&L)

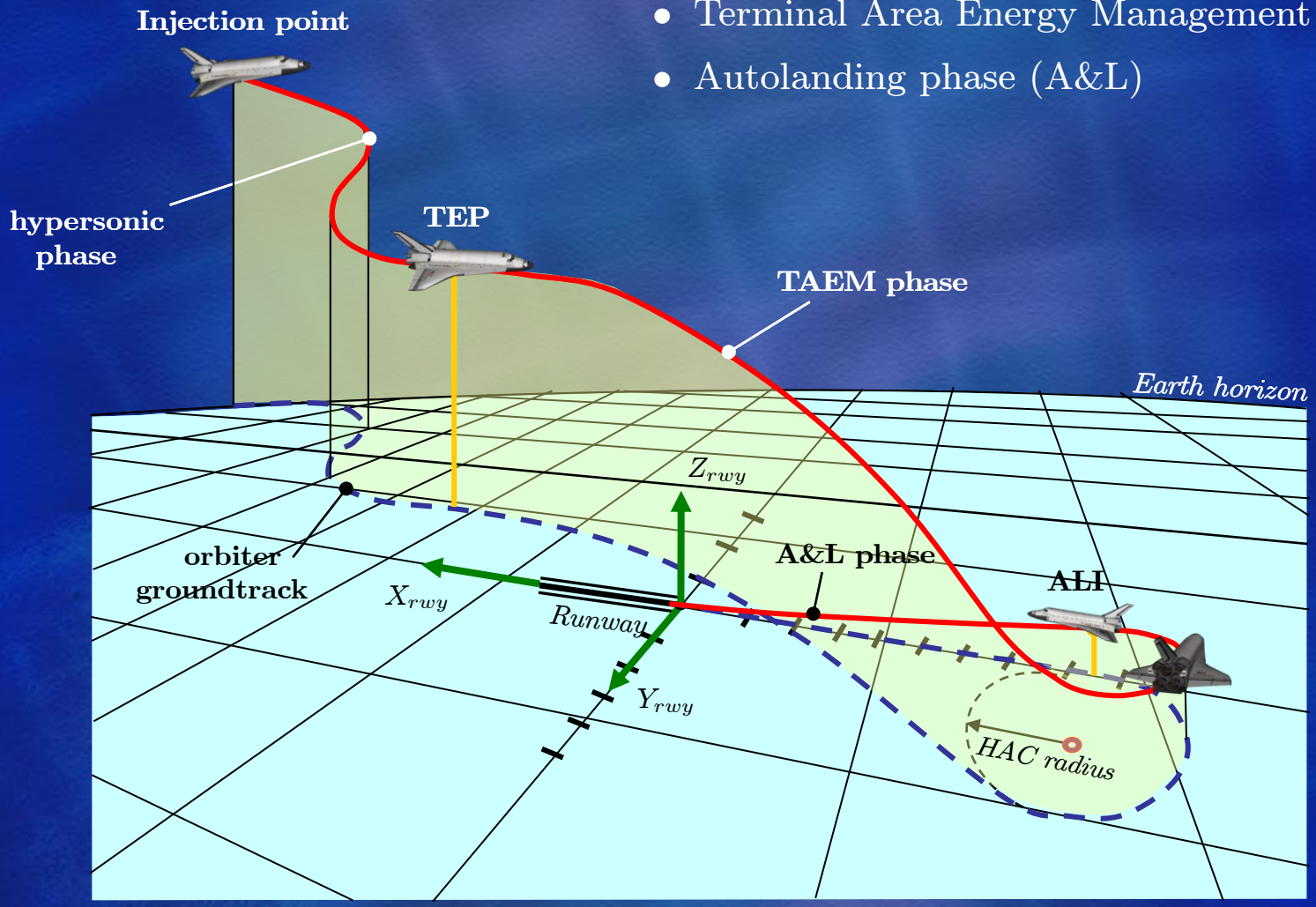

sketch of an atmospheric reentry mission

TAEM guidance problem

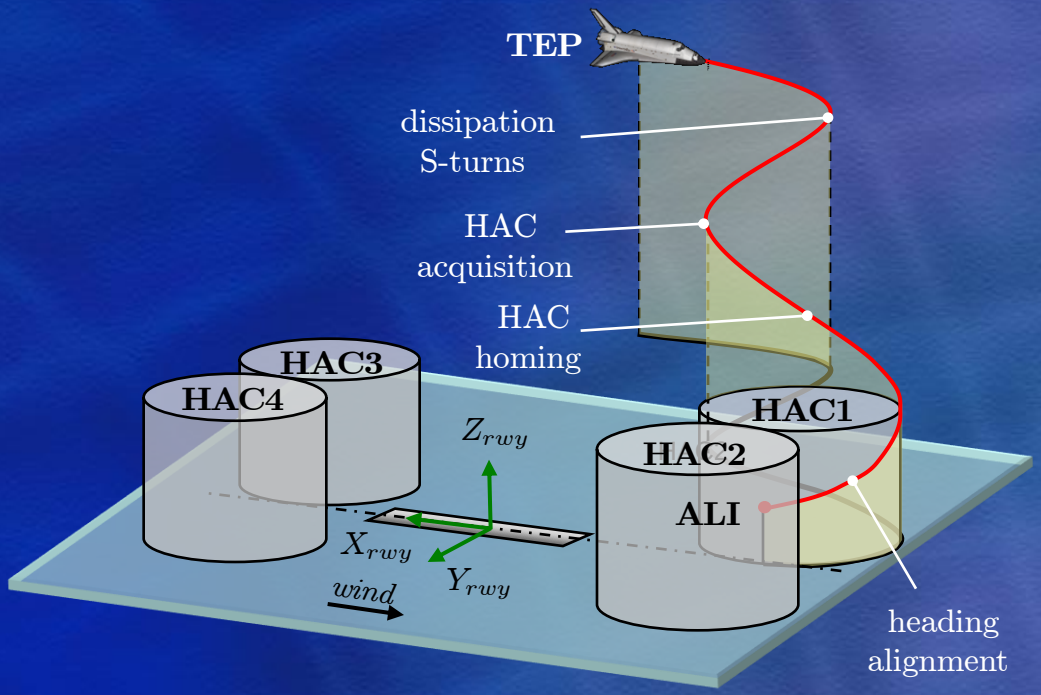

	requirements
mechanical constraints	
max. load factor $\Gamma_{\max}$ $[g]$	< 2.5
max. dynamic pressure $\overline{q}_{\max}$ $[kPa]$	< 16
kinematic constraints at ALI	
Mach number	0.5
altitude $[km]$	5
downrange $[km]$	10
crossrange $[km]$	0
final heading $[deg]$	headwind landing
flight path angle $[deg]$	-27

TAEM guidance constraints

	α	μ	β
lower bound $[deg]$	0	-80	-3
upper bound $[deg]$	25	80	3
max. rate $[deg/s]$	2	5	2

guidance inputs bounds and rates

Objectives:

- dissipate the total energy of the vehicle from entry point (TEP) down to nominal exit point (ALI)
- align the vehicle with the extended runway centerline to ensure a safe autolanding

2 kinds of constraints:

- *trajectory constraints:* dynamic pressure, load factor
- *mission constraints:* kinematic constraints at ALI

TAEM guidance problem

- 3 dof model in flat Earth coordinates:

position

$$\begin{cases} \dot{x} = V\cos\chi\cos\gamma, \\ \dot{y} = V\sin\chi\cos\gamma, \\ \dot{h} = V\sin\gamma. \end{cases}$$

velocity

$$\begin{cases} \dot{V} = -\dfrac{D(\alpha,M)}{m} - g\sin\gamma, \\ \dot{\gamma} = \dfrac{1}{mV}\left(L(\alpha,M)\cos\mu - Y(\beta,M)\sin\mu\right) - \dfrac{g}{V}\cos\gamma, \\ \dot{\chi} = \dfrac{1}{mV\cos\gamma}\left(L(\alpha,M)\sin\mu + Y(\beta,M)\cos\mu\right). \end{cases}$$

where $L(\alpha,M) = \overline{q}SC_{L_0}(\alpha,M)$, $D(\alpha,M) = \overline{q}SC_{D_0}(\alpha,M)$, $Y(\beta,M) = \overline{q}SC_{Y_0}(\beta,M)$.

and $\overline{q} = \frac{1}{2}\rho V^2$: dynamic pressure, g: constant gravitational acceleration, $\rho = \rho_0 exp\,(-h/H_0)$: atmospheric density.

- the corresponding optimal control problem is given (in the state space) by:

$$\min_{x(t),u(t)} \quad \mathcal{C}_0\left(x(t_0),u(t_0)\right) + \int_{t_0}^{tf} \mathcal{C}_t\left(x(t),u(t)\right)dt + \mathcal{C}_f\left(x(t_f),u(t_f)\right)$$

t.q.

$$\begin{aligned} \dot{x}(t) &= f\left(x(t),u(t)\right), && t\in[t_0,t_f], \\ x(t_0) &= x_0, \\ u(t_0) &= u_0, \\ 0 \le\ & \Gamma\left(x(t),u(t)\right) \le \Gamma_{\max}, && t\in[t_0,t_f], \\ 0 \le\ & \overline{q}(x(t)) \le \overline{q}_{\max}, && t\in[t_0,t_f], \\ u_{\min} \le\ & u(t) \le u_{\max}, && t\in[t_0,t_f], \\ x(t_f) &= x_f, \\ u(t_f) &= u_f. \end{aligned}$$

A&L guidance problem

Objectives:

- bring the vehicle from ALI point down to wheels stop on the runway
- simpler problem than TAEM (longitudinal motion only)

Constraints:

- similar to TAEM phase

	requirements
mechanical constraints	
max. load factor $\Gamma_{\max}$ $[g]$	< 2.5
max. dynamic pressure $\overline{q}_{\max}$ $[kPa]$	< 16
kinematic constraints at touchdown	
relative velocity $[m/s]$	90
altitude $[km]$	runway altitude
downrange $[km]$	0
flight path angle $[deg]$	-3

A&L guidance constraints

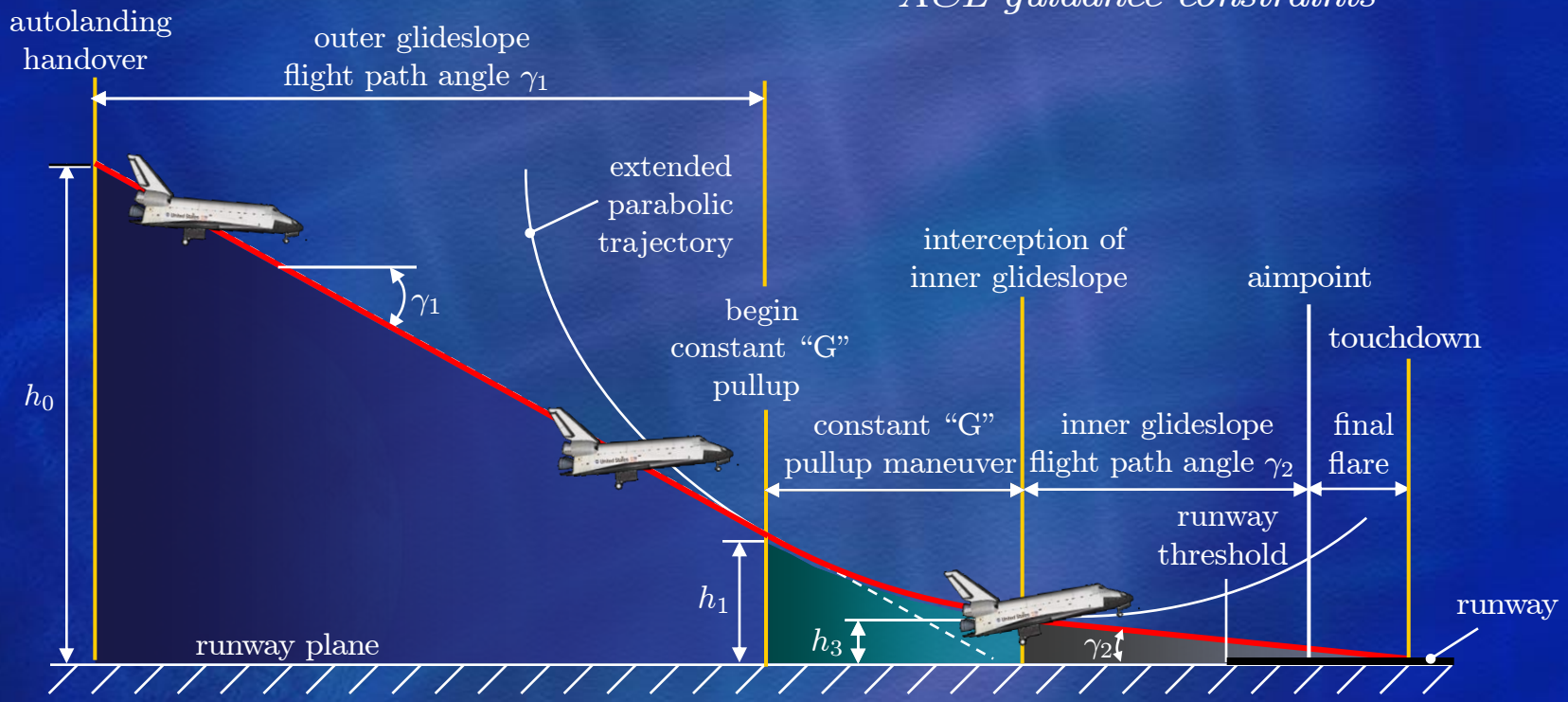

A&L trajectory profile

- 3 dof equations of motion in flat Earth coordinates are given by

$$\begin{cases} \dot{x} = V\cos\gamma, \\ \dot{h} = V\sin\gamma, \\ \dot{V} = -\dfrac{D(\alpha,M)}{m} - g\sin\gamma, \\ \dot{\gamma} = \dfrac{L(\alpha,M)}{mV} - \dfrac{g}{V}\cos\gamma, \end{cases}$$

where $\overline{q} = \frac{1}{2}\rho V^2$ and $\Gamma = \dfrac{\sqrt{L^2(\alpha,M)+D^2(\alpha,M)}}{mg}$: total load factor.

- the corresponding optimal control problem is given (in the state space) by:

$$\min_{x(t),u(t)} \quad \mathcal{C}_0\left(x(t_0),u(t_0)\right) + \int_{t_0}^{tf} \mathcal{C}_t\left(x(t),u(t)\right)dt + \mathcal{C}_f\left(x(t_f),u(t_f)\right)$$

t.q.

$$\begin{array}{ccccc} & & \dot{x}(t) = f\left(x(t),u(t)\right), & & t\in[t_0,t_f], \\ & & x(t_0) = x_0, & & \\ & & u(t_0) = u_0, & & \\ 0 & \leq & \Gamma\left(x(t),u(t)\right) & \leq & \Gamma_{\max}, \quad t\in[t_0,t_f], \\ 0 & \leq & \overline{q}(x(t)) & \leq & \overline{q}_{\max}, \quad t\in[t_0,t_f], \\ u_{\min} & \leq & u(t) & \leq & u_{\max}, \quad t\in[t_0,t_f], \\ & & x(t_f) = x_f, & & \\ & & u(t_f) = u_f. & & \end{array}$$

Part II
Autonomous guidance law architecture

Autonomous guidance law: main objectives

Objectives:

- *Design of an autonomous guidance law for atmospheric reentry vehicles*
- provide a level of fault tolerance against severe aerodynamic control surfaces failures
- onboard processing to react quickly to manage a faulty situation
- provide high levels of performance and robustness

Motivation:

- to improve in-service guidance schemes by locally assigning autonomy and responsibility to the vehicle, exempting the ground segment from "low level" operational tasks, so that it can ensure more efficiently its mission of global coordination

Methodological approach:

- use *flatness approach* as the baseline tool to perform onboard processing
- atmospheric reentry trajectory planning/reshaping in faulty situations
- integration of static aerologic disturbances
- convexification of the optimal control problem to guarantee convergence

Constraints:

- reliable FDI indicators

Autonomous guidance law: functional architecture

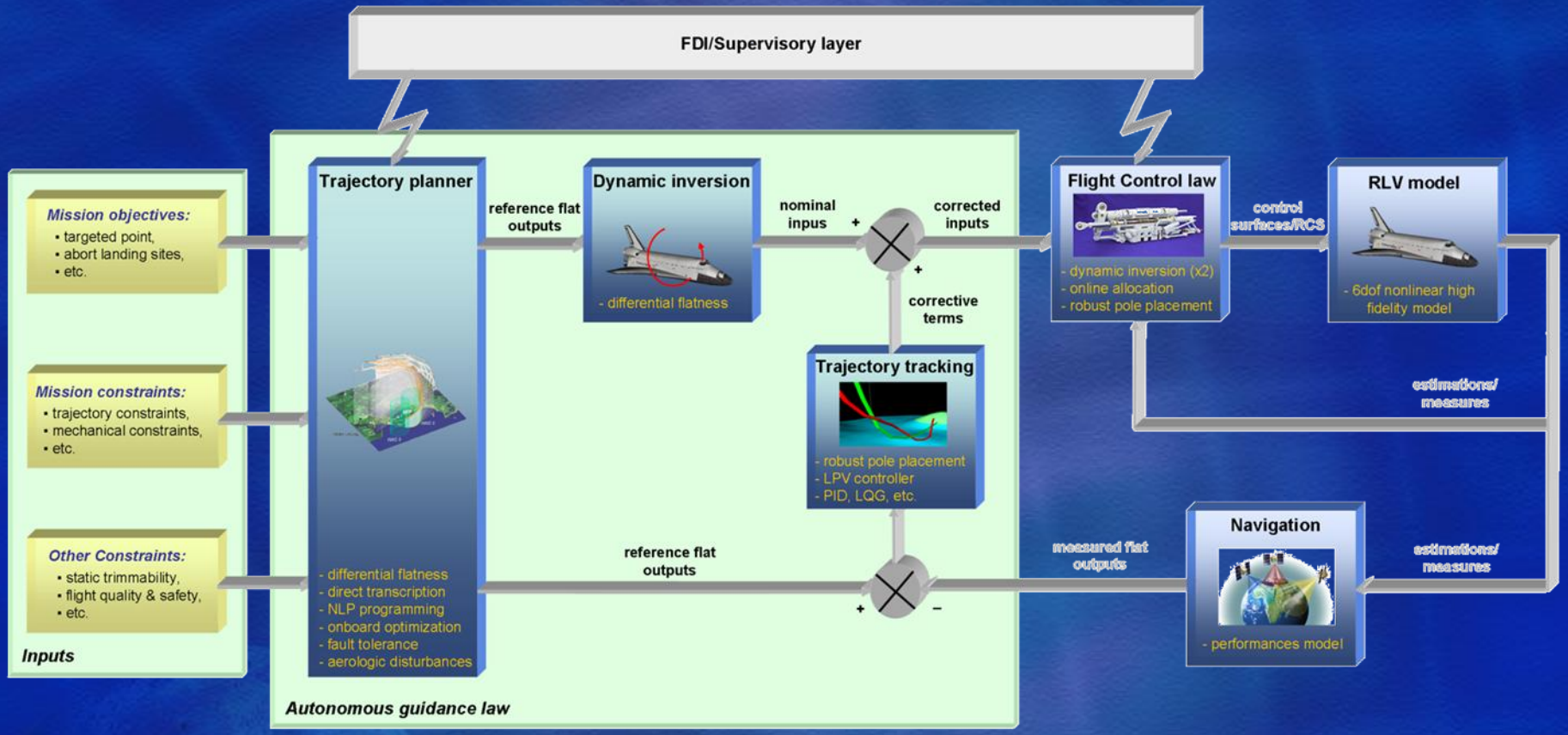

functional architecture of the autonomous guidance law

The proposed autonomous guidance law consists of:

- a Fault-Tolerant Onboard Path Planner (FTOPP)
- a Nonlinear Dynamic Inversion block based on flatness approach
- a trajectory tracking controller (LPV controller, not presented)

This presentation focus on the design of the FTOPP and the NDI functions

Part III
Flatness-based trajectory planning

Advantages of flatness approach for trajectory planning applications

- *minimum number of decision variables in the OCP:* the optimization variables become the flat output of the system
- *integration-free optimization problem:* the system dynamics is intrinsically satisfied
- avoid emergence of *unobservable dynamics* (which may be potentially unstable)

Main drawback:

- often highly nonlinear and nonconvex OCP in the flat output space

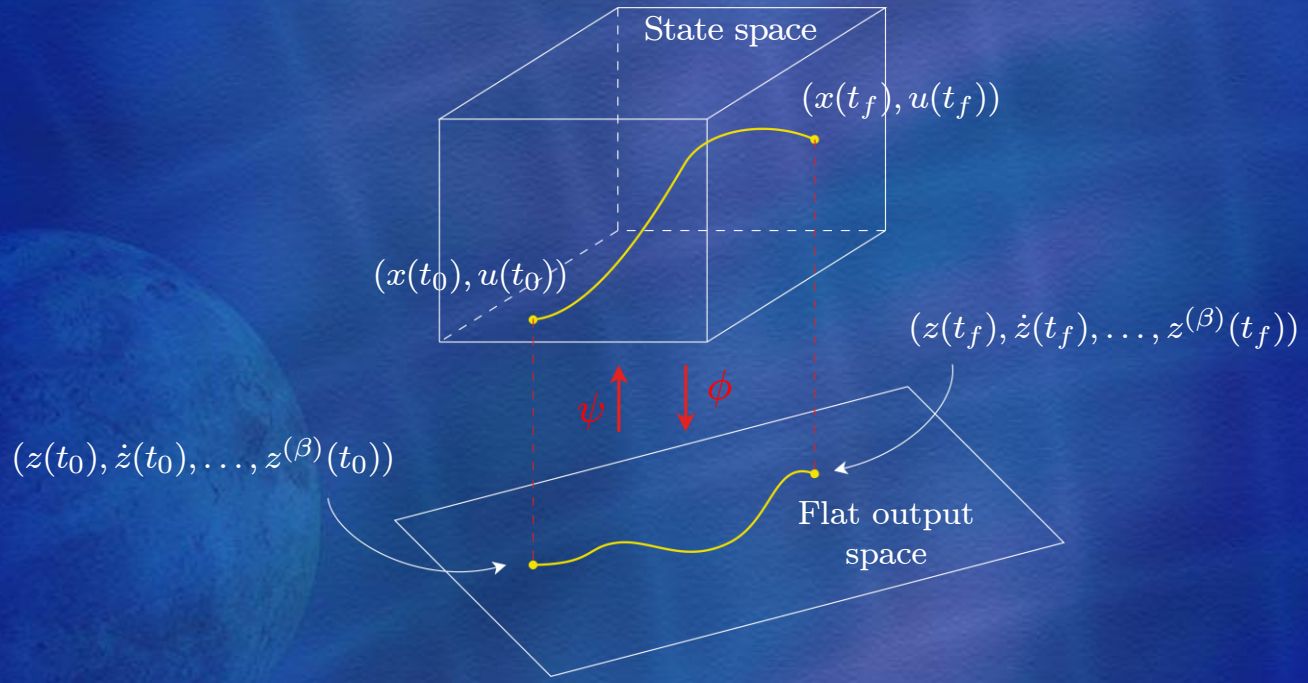

equivalence between system trajectories

- *Differential flatness* concept introduced in 1991 by Fliess, Lévine, Martin and Rouchon: deals with "pseudo" nonlinear systems

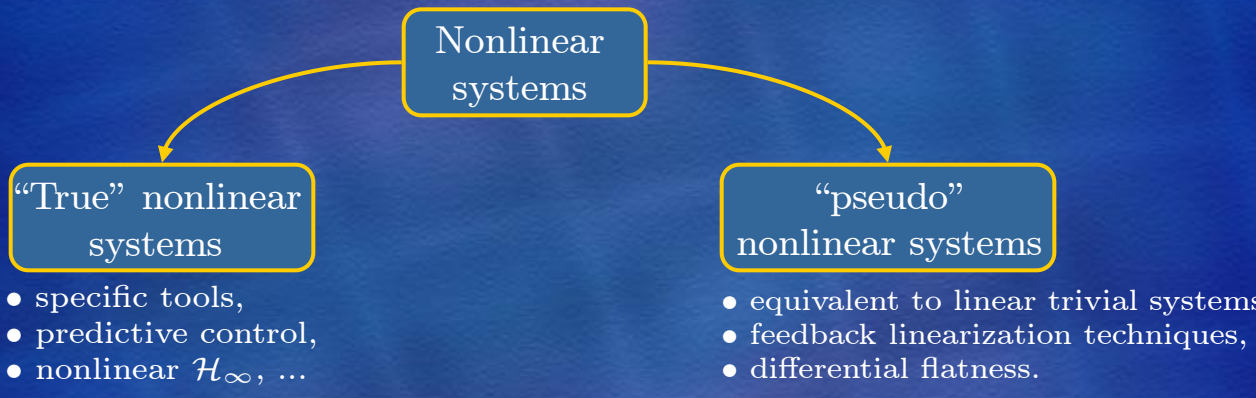

Definition (Differential flatness (Fliess *et al.*, 1995))**.** *The nonlinear system* $\dot{x} = f(x,u)$ *is* differentially flat *(or, shortly flat) if and only if there exists a collection* z *of* m *variables, whose elements are differentially independant, defined by:*

$$z = \phi\left(x, u, \dot{u}, \ldots, u^{(\alpha)}\right),$$

such that

$$\begin{cases} x = \psi_x\left(z, \dot{z}, \ldots, z^{(\beta-1)}\right) \\ u = \psi_u\left(z, \dot{z}, \ldots, z^{(\beta)}\right) \end{cases}$$

where ψ_x *and* ψ_u *are smooth applications over the manifold* X*, and* $\alpha = (\alpha_1, \ldots, \alpha_m)$*,* $\beta = (\beta_1, \ldots, \beta_m)$ *are finite* m*-tuples of integers.*

The collection $z \in \mathbb{R}^m$ *is called a* flat output *(or linearizing output).*

A simple example

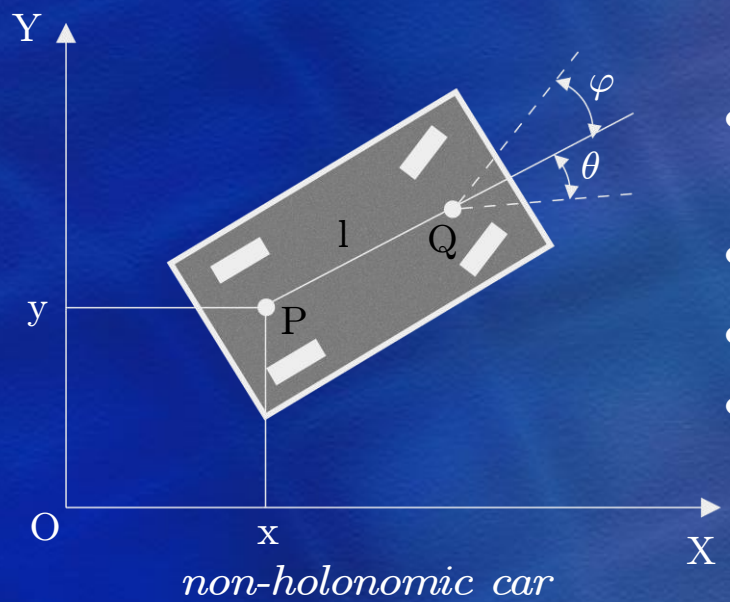

non-holonomic car

- kinematic equations:

$$\begin{cases} \dot{x} = u\cos\theta \\ \dot{y} = u\sin\theta \\ \dot{\theta} = \dfrac{u}{l}\tan\varphi \end{cases}$$

- implicit form: $\dot{x}\sin\theta - \dot{y}\cos\theta = 0$
- candidate flat output: (x, y)
- state and inputs wrt the flat output and its derivatives:

$$\theta = \arctan\left(\frac{\dot{y}}{\dot{x}}\right), u = \sqrt{\dot{x}^2 + \dot{y}^2}, \varphi = \arctan\left(\frac{l(\ddot{y}\dot{x} - \dot{y}\ddot{x})}{(\dot{x}^2 + \dot{y}^2)^{\frac{3}{2}}}\right)$$

Flatness necessary and sufficient conditions

- General formulations of flatness necessary and sufficient conditions are now well-established for linear and nonlinear systems governed by ordinary differential equations (Lévine and Nguyen (2003), Lévine (2006))
- Based on classical tools coming from linear polynomial algebra: *Smith decompositions*
- Cartan's generalized *moving frame structure equations* are used to find an integrable basis

- Theoretical contribution to flatness theory
- Joint work with Prof. Jean Lévine at the Centre Automatique et Systèmes (CAS), École des Mines de Paris, France.
- Extension of the results obtained for linear systems governed by ordinary differential equations
- Development of a simple constructive algorithm to check if a linear system is δ-flat and, if so, to compute a candidate δ-flat output:
  - Based on classical concepts coming from linear polynomial algebra: *Smith decompositions*
  - The system is considered in *implicit form* to account for its natural property of invariance by endogenous dynamic feedback
- See PhD dissertation for more details
- A journal paper under preparation

- Consider a nonlinear system defined on a differentiable manifold by

$$\dot{x}(t) = f\left(x(t), u(t)\right),$$

where $x : [t_0, t_f] \mapsto \mathbb{R}^n$: state of size n and $u : [t_0, t_f] \mapsto \mathbb{R}^m$: control inputs vector of size m.

- We consider that all the the trajectory planning objectives, defined either at the "mission" level or at the "vehicle" level, may be classically formulated as a constrained optimal control problem (OCP)

$$\min_{x(t),u(t)} \quad \mathcal{C}_0\left(x(t_0), u(t_0, t_0)\right) + \int_{t_0}^{t_f} \mathcal{C}_t\left(x(t), u(t), t\right) dt + \mathcal{C}_f\left(x(t_f), u(t_f), t_f\right)$$

s.t.

$$\begin{array}{rcccll}
 & & \dot{x}(t) = f\left(x(t), u(t)\right), & & & t \in [t_0, t_f], \\
l_0 & \leq & A_0 x(t_0) + B_0 u(t_0) & \leq & u_0, & \\
l_t & \leq & A_t x(t) + B_t u(t) & \leq & u_t, & t \in [t_0, t_f], \\
l_f & \leq & A_f x(t_f) + B_f u(t_f) & \leq & u_f, & \\
L_0 & \leq & c_0\left(x(t_0), u(t_0)\right) & \leq & U_0, & \\
L_t & \leq & c_t\left(x(t), u(t)\right) & \leq & U_t, & t \in [t_0, t_f], \\
L_f & \leq & c_f\left(x(t_f), u(t_f)\right) & \leq & U_f. &
\end{array}$$

- the *equivalent* optimal control problem in the flat output space is given by

$$\min_{\overline{z}(t)} \quad \mathcal{C}_0\left(\psi_x(\overline{z}(t_0)), \psi_u(\overline{z}(t_0)), t_0\right) + \int_{t_0}^{t_f} \mathcal{C}_t\left(\psi_x(\overline{z}(t)), \psi_u(\overline{z}(t)), t\right) dt$$
$$+\mathcal{C}_f\left(\psi_x(\overline{z}(t_f)), \psi_u(\overline{z}(t_f)), t_f\right)$$

s.t.

$$\begin{array}{ccccc} l_0 & \leq & A_0\overline{z}(t_0) & \leq & u_0, \\ l_t & \leq & A_t\overline{z}(t) & \leq & u_t, \qquad t \in [t_0, t_f], \\ l_f & \leq & A_f\overline{z}(t_f) & \leq & u_f, \\ L_0 & \leq & c_0\left(\psi_x(\overline{z}(t_0)), \psi_u(\overline{z}(t_0))\right) & \leq & U_0, \\ L_t & \leq & c_t\left(\psi_x(\overline{z}(t)), \psi_u(\overline{z}(t))\right) & \leq & U_t, \qquad t \in [t_0, t_f], \\ L_f & \leq & c_f\left(\psi_x(\overline{z}(t_f)), \psi_u(\overline{z}(t_f))\right) & \leq & U_f. \end{array}$$

where the flat output

$$z = \phi\left(x, u, \dot{u}, \ldots, u^{(\alpha)}\right)$$

satisfies

$$\begin{cases} x = \psi_x\left(z, \dot{z}, \ldots, z^{(\beta-1)}\right), \\ u = \psi_u\left(z, \dot{z}, \ldots, z^{(\beta)}\right). \end{cases}$$

- OCP decision variables: $\overline{z} = (z_1, \ldots, z_m, \dot{z}_1, \ldots, \dot{z}_m, \ldots, z_1^{(2)}, \ldots, z_m^{(2)}, \ldots)$

1) parametrization of the OCP decision variables by means of B-spline curves

$$
\begin{aligned}
z_1(t, p^1) &= \sum_{i=0}^{q_1} c_i^1 \mathcal{B}_{i,k_1}(t) && \text{for the knot breakpoint sequence } \eta_1, \\
z_2(t, p^2) &= \sum_{i=0}^{q_2} c_i^2 \mathcal{B}_{i,k_2}(t) && \text{for the knot breakpoint sequence } \eta_2, \\
&\vdots \\
z_m(t, p^m) &= \sum_{i=0}^{q_m} c_i^m \mathcal{B}_{i,k_m}(t) && \text{for the knot breakpoint sequence } \eta_m,
\end{aligned}
$$

where $\mathcal{B}_{i,k_j}(t)$ is the zero order derivative of the i-th function associated to the B-spline basis of order k_j, built on the knot breakpoint sequence η_j, and c_i^j is the corresponding vector of control points.

2) discretization of the optimal control problem over the time partition

$$t_0 = \tau_1 < \tau_2 < \tau_N = t_f,$$

where N is a predefined number of collocation points.

The cost functional is approximated by means of a quadrature rule.

We obtain a sparse collocation matrix such that

$$
\begin{bmatrix}
z_i^{(0)}(\tau_0) \\ z_i^{(1)}(\tau_0) \\ \vdots \\ z_i^{(\beta_i)}(\tau_0) \\
z_i^{(0)}(\tau_1) \\ z_i^{(1)}(\tau_1) \\ \vdots \\ z_i^{(\beta_i)}(\tau_1) \\
z_i^{(0)}(\tau_2) \\ z_i^{(1)}(\tau_2) \\ \vdots \\ z_i^{(\beta_i)}(\tau_2) \\
z_i^{(0)}(\tau_3) \\ z_i^{(1)}(\tau_3) \\ \vdots \\ z_i^{(\beta_i)}(\tau_3) \\
\vdots \\
z_i^{(0)}(\tau_{N-1}) \\ z_i^{(1)}(\tau_{N-1}) \\ \vdots \\ z_i^{(\beta_i)}(\tau_{N-1}) \\
z_i^{(0)}(\tau_N) \\ z_i^{(1)}(\tau_N) \\ \vdots \\ z_i^{(\beta_i)}(\tau_N)
\end{bmatrix}
=
\left[
\begin{array}{cccccccccccccccc}
\star & & & & & & & & & & & & & & & \\
\star & \star & & & & & & & & & & & & & & \\
\vdots & & \ddots & & & & & & & & & & & & & \\
\star & \star & \cdots\star & & & & & & & & & & & & & \\
\star & \star & \star & \cdots\star & \star & \cdots\star & & & & & & & & & & \\
\star & \star & \star & \cdots\star & \star & \cdots\star & & & & & & & & & & \\
\vdots & & & \vdots & \vdots & \vdots & & & & & & & & & & \\
\star & \star & \star & \cdots\star & \star & \cdots\star & & & & & & & & & & \\
 & & & & \star & \star & \star & \cdots\star & \star & \cdots\star & & & & & & \\
 & & & & \star & \star & \star & \cdots\star & \star & \cdots\star & & & & & & \\
 & & & & \vdots & & & \vdots & \vdots & \vdots & & & & & & \\
 & & & & \star & \star & \star & \cdots\star & \star & \cdots\star & & & & & & \\
 & & & & \star & \star & \star & \cdots\star & \star & \cdots\star & & & & & & \\
 & & & & \star & \star & \star & \cdots\star & \star & \cdots\star & & & & & & \\
 & & & & \vdots & & & \vdots & \vdots & \vdots & & & & & & \\
 & & & & \star & \star & \star & \cdots\star & \star & \cdots\star & & & & & & \\
 & & & & & & & & & & \ddots & \ddots & & & & \\
 & & & & & & & & & & \star & \star & \star & \cdots\star & \star & \cdots\star \\
 & & & & & & & & & & \star & \star & \star & \cdots\star & \star & \cdots\star \\
 & & & & & & & & & & \vdots & & & \vdots & \vdots & \vdots \\
 & & & & & & & & & & \star & \star & \star & \cdots\star & \star & \cdots\star \\
 & & & & & & & & & & & & & & & \star \\
 & & & & & & & & & & & & & & \star & \star \\
 & & & & & & & & & & & & & & & \vdots \\
 & & & & & & & & & & & & & \star & \cdots\star & \star
\end{array}
\right]
\begin{bmatrix}
c_1^i \\ c_2^i \\ c_{k_i-s_i}^i \\ c_{k_i-s_i+1}^i \\ \vdots \\
c_{2(k_i-s_i)}^i \\ c_{2(k_i-s_i)+1}^i \\ \vdots \\
c_{l_i(k_i-s_i)}^i \\ c_{l_i(k_i-s_i)+1}^i \\ \vdots \\
c_{l_i(k_i-s_i)+s_i}^i
\end{bmatrix}
$$

Direct transcription into an NLP problem

- by setting $u_i \triangleq \left(c_1^i, c_2^i, \ldots, c_{l_i(k_i-s_i)+s_i}^i\right) \in \mathbb{R}^{l_i(k_i-s_i)+s_i}$, the set of all control points of the B-splines can be defined by

$$u \triangleq (u_1, \ldots, u_m)\,.$$

- the OCP constraints, evaluated at every collocation points are given by

$$\Lambda(u) = \left(\Lambda_{li}(u), \Lambda_{nli}(u), \Lambda_{lt}^1(u), \ldots, \Lambda_{lt}^N(u), \Lambda_{nlt}^1(u), \ldots, \Lambda_{nlt}^N(u), \Lambda_{lf}(u), \Lambda_{nlf}(u)\right),$$

$$\begin{cases} \Lambda_{lt}^j(u) &= A_t \overline{z}(t_j), & j = 1, \ldots, N, \\ \Lambda_{nlt}^j(u) &= c_t\left(\psi_x(\overline{z}(t_j)), \psi_u(\overline{z}(t_j))\right), & j = 1, \ldots, N, \\ \Lambda_{li}(u) &= A_0 \overline{z}(t_0), \\ \Lambda_{lf}(u) &= A_f \overline{z}(t_f), \\ \Lambda_{nli}(u) &= c_0\left(\psi_x(\overline{z}(t_0)), \psi_u(\overline{z}(t_0))\right), \\ \Lambda_{nlf}(u) &= c_f\left(\psi_x(\overline{z}(t_f)), \psi_u(\overline{z}(t_f))\right). \end{cases}$$

- the B-splines control points become the new decision variables of the nonlinear programming (NLP) problem

$$\begin{aligned} &\min_{u \in \mathbb{R}^M} && J(u) \\ &\text{s.t.} && L_b \leq \Lambda(u) \leq U_b, \\ &\text{where } M = \sum_{i=1}^{m} l_i(k_i - s_i) + s_i. \end{aligned}$$

- the NLP problem can be solved onboard by using NPSOL, SNOPT, KNITRO, ...

Assumptions:

- flat Earth: coriolis and centrifugal forces neglected,
- symetric flight: $\beta = 0$ (typical guidance assumption),
- no cost functional considered: feasibility problem only

Tabulated aerodynamic force coefficients in clean configuration are approximated by means of:

- principal component analysis (PCA): *results in a decoupling of angle-of-attack and Mach number variables*,
- analytical neural networks (ANN): *parcimonious approximators of smooth multivariate functions*

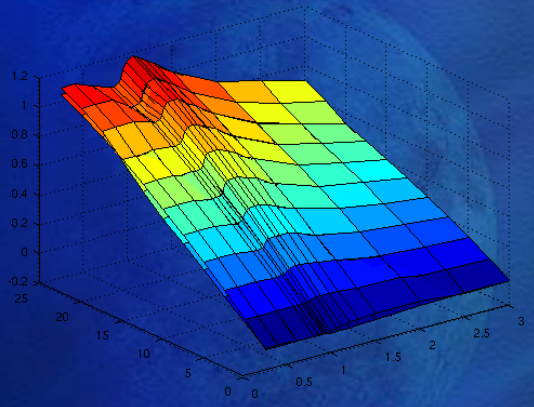

lift coefficient C_{L_0}

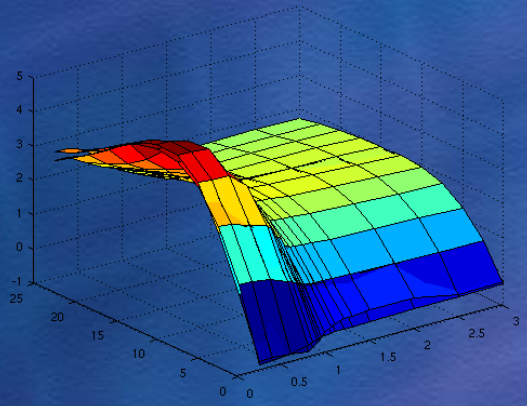

gliding ratio C_{L_0}/C_{D_0}

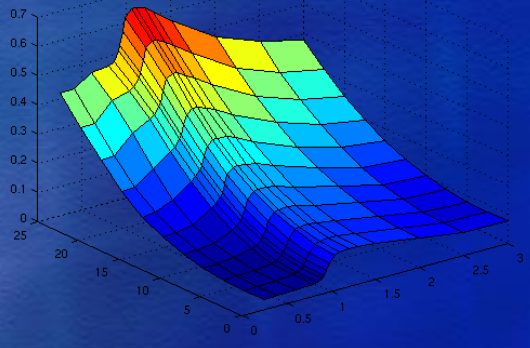

drag coefficient C_{D_0}

- time being not a relevant parameter during atmospheric reentry, the 3 dof model is reparameterized wrt. free trajectory duration parameter λ

$$\tau = \frac{t}{\lambda}, \text{ with } 0 \cdot \ \tau \cdot \ 1\text{: normalized time} \quad \Longrightarrow \quad (.)' = \frac{d(.)}{d\tau} = \lambda \frac{d(.)}{dt},$$

- the new point-mass model is given by

position

$$\begin{cases} x' = \lambda V \cos\chi \cos\gamma, \\ y' = \lambda V \sin\chi \cos\gamma, \\ h' = \lambda V \sin\gamma. \end{cases}$$

velocity

$$\begin{cases} V' = \lambda \left(-\dfrac{D}{m} - g \sin\gamma \right), \\ \gamma' = \lambda \left(\dfrac{L \cos\mu}{mV} - \dfrac{g}{V} \cos\gamma \right), \\ \chi' = \lambda \dfrac{L \sin\mu}{mV \cos\gamma}. \end{cases}$$

- this model is <u>not flat</u> since $\beta = 0$, but the autonomous observable may be parameterized wrt. $z_1 = x$, $z_2 = y$ and $z_3 = h$ and the parameter λ

<u>states:</u>

$$V = \frac{\sqrt{z_1'^2 + z_2'^2 + z_3'^2}}{\lambda}, \qquad V' = \frac{z_1' z_1'' + z_2' z_2'' + z_3' z_3''}{\lambda \sqrt{z_1'^2 + z_2'^2 + z_3'^2}},$$

$$\gamma = \arctan\left(\frac{z_3'}{\sqrt{z_1'^2 + z_2'^2}} \right), \qquad \gamma' = \frac{z_3''(z_1'^2 + z_2'^2) - z_3'(z_1' z_1'' + z_2' z_2'')}{(z_1'^2 + z_2'^2 + z_3'^2)\sqrt{z_1'^2 + z_2'^2}},$$

$$\chi = \arctan\left(\frac{z_2'}{z_1'} \right), \qquad \chi' = \frac{z_2'' z_1' - z_2' z_1''}{z_1'^2 + z_2'^2}.$$

inputs: $\mu = \arctan\left(\dfrac{\chi' \cos\gamma}{\gamma' + \dfrac{g\cos\gamma}{V}\lambda}\right)$, $\alpha = \dfrac{2m}{a_1 f_{C_{L_0}}(M)\rho S V \cos\mu}\left(\dfrac{\gamma'}{\lambda} + \dfrac{g\cos\gamma}{V}\right) - \dfrac{a_0}{a_1}$,

where $C_{L_0}(\alpha, M) = (a_0 + a_1\alpha) f_{C_{L_0}}(M)$,

equality constraint: $\Lambda_\tau(x,u) = \dfrac{V'}{\lambda} + g\sin\gamma + \dfrac{1}{2}\dfrac{\rho S V^2 C_{D_0}(\alpha, M)}{m} = 0$,

The corresponding optimal control problem in the flat output space is given by

find $(\overline{z}(t), \lambda)$

s.t.

$$
\begin{array}{ccccc}
 & & \psi_x(\overline{z}(\tau_0), \lambda) = x_0, & & \\
 & & \psi_u(\overline{z}(\tau_0), \lambda) = u_0, & & \\
 & & \Lambda_\tau(\psi_x(\overline{z}(\tau), \psi_u(\overline{z}(\tau), \lambda) = 0, & & \tau \in [\tau_0, \tau_f], \\
0 & \leq & \Gamma\left(\psi_x(\overline{z}(\tau), \lambda), \psi_u(\overline{z}(\tau), \lambda)\right) & \leq & \Gamma_{\max}, \quad \tau \in [\tau_0, \tau_f], \\
0 & \leq & \overline{q}(\psi_x(\overline{z}(\tau), \lambda) & \leq & \overline{q}_{\max}, \quad \tau \in [\tau_0, \tau_f], \\
u_{\min} & \leq & \psi_u(\overline{z}(\tau), \lambda) & \leq & u_{\max}, \quad \tau \in [\tau_0, \tau_f], \\
 & & \psi_x(\overline{z}(\tau_f), \lambda) = x_f, & & \\
 & & \psi_u(\overline{z}(\tau_f), \lambda) = u_f, & &
\end{array}
$$

where $\overline{z} = (z_1, z_2, z_3, \dot{z}_1, \dot{z}_2, \dot{z}_3, \ddot{z}_1, \ddot{z}_2, \ddot{z}_3)$, $\tau_0 = 0$ and $\tau_f = 1$.

Monte Carlo simulations results (NLP solver: NPSOL)

parameter	**symbol**	**nominal value**	σ
Position			
initial downrange $[km]$	x_0	-20	± 7
initial crossrange $[km]$	y_0	-30	± 7
initial altitude $[km]$	h_0	25	± 3
Velocity			
initial Mach number	M_0	2	N.A.
initial flight path angle $[deg]$	γ_0	-5	± 2
initial heading $[deg]$	χ_0	-30	± 10

initial kinematic conditions at TEP

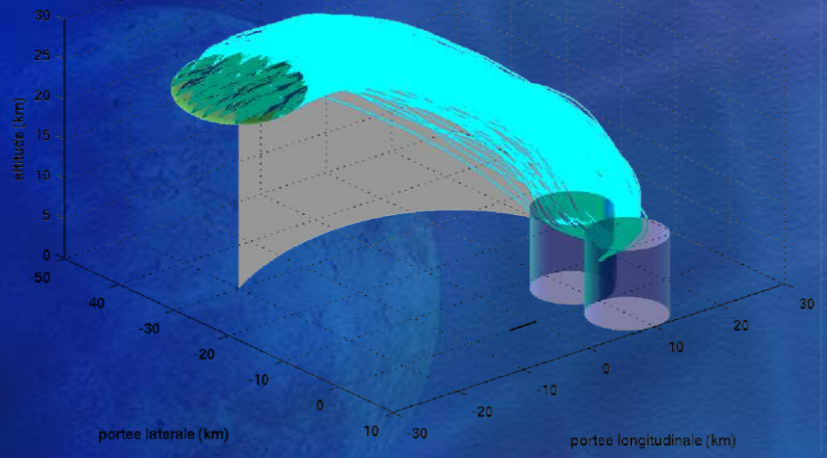

3D reference trajectories

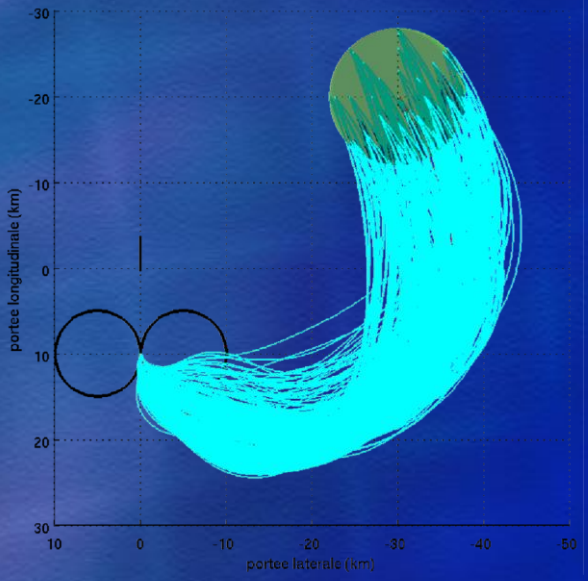

projection in the horizontal plane

Monte Carlo simulations results:

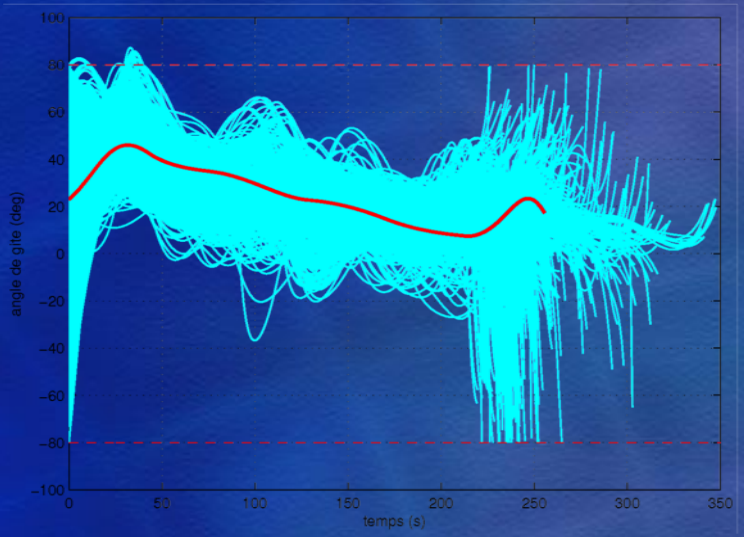

reference bank angle profiles

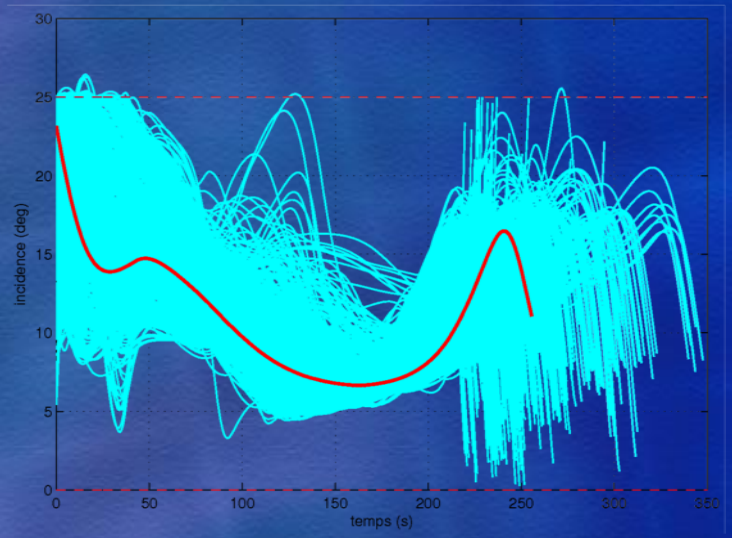

reference angle-of-attack profiles

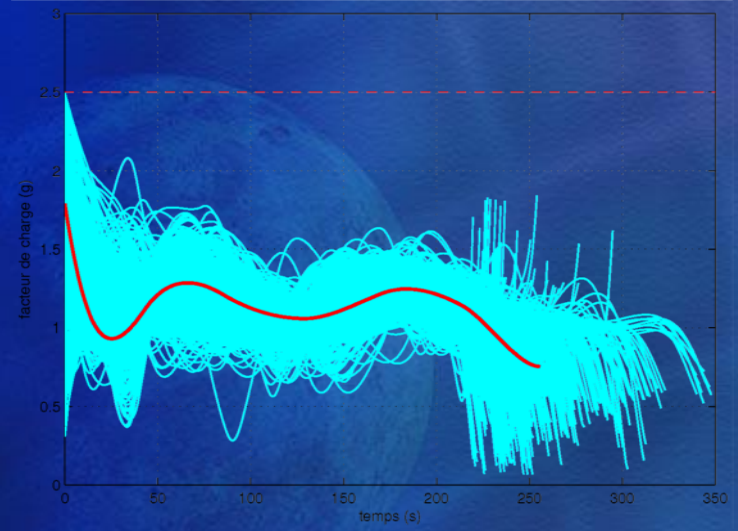

reference load factor profiles

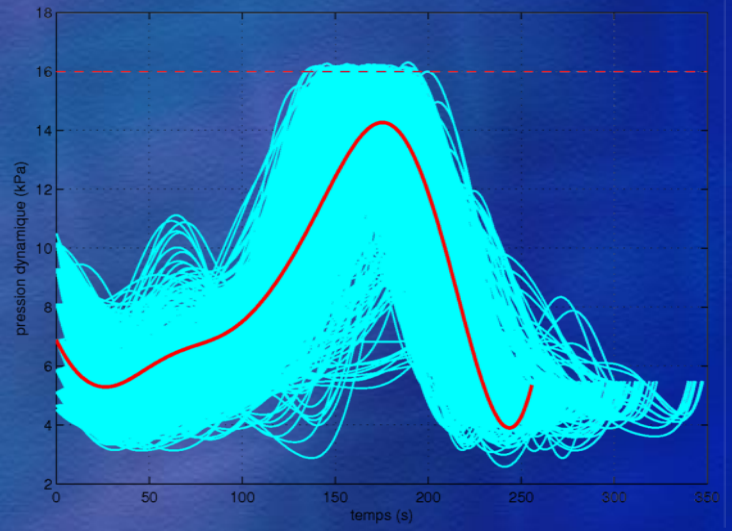

reference dynamic pressure profiles

Monte Carlo simulations results:

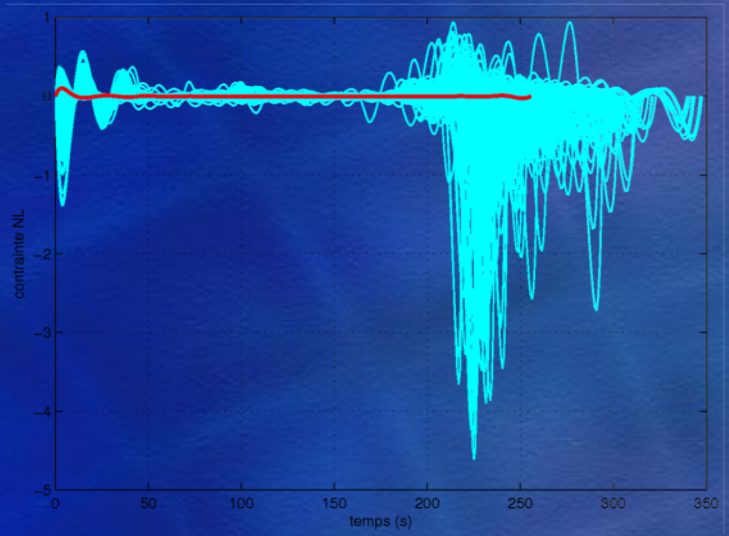

reference equality constraint profiles

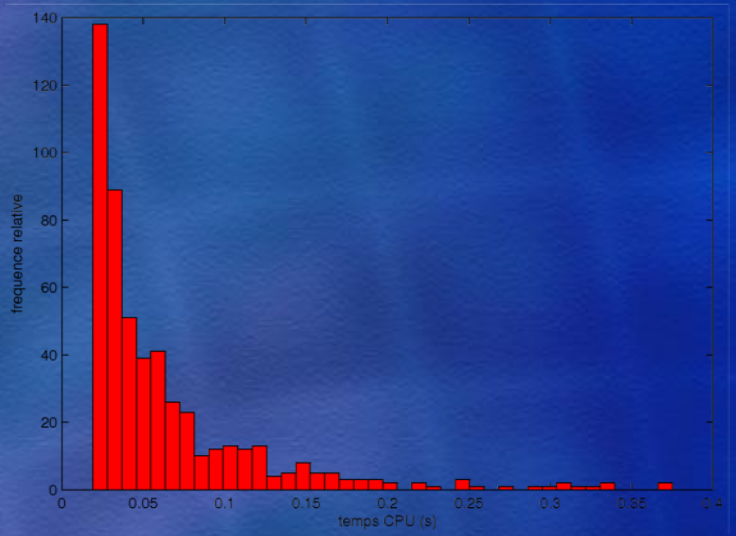

CPU time: probability distribution

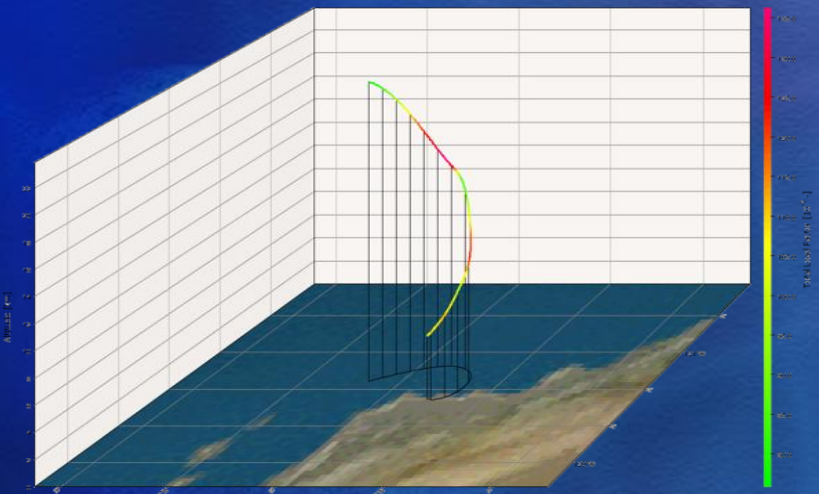

TAEM trajectory obtained with ASTOS

Comparison with ASTOS tool:

- optimization time: 36.5 s with the baseline tuning,
- flatness-based approach: 0.37 s in the worst case ($\approx$ 100 times faster)

Parametrization wrt. total energy (see PhD dissertation)

- parametrization of the longitudinal model wrt. the downrange x

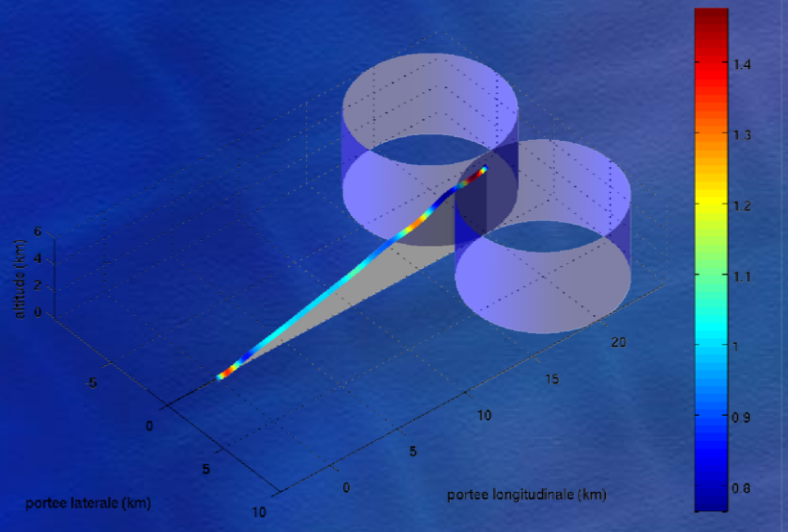

3D reference trajectory

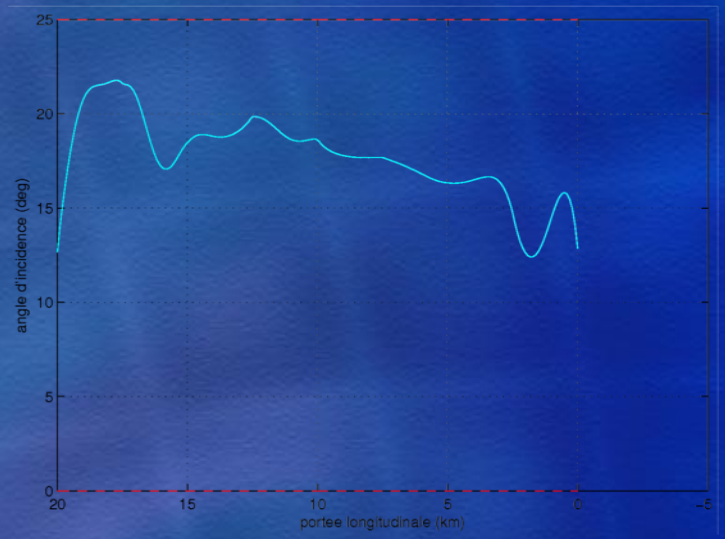

angle-of-attack reference profile

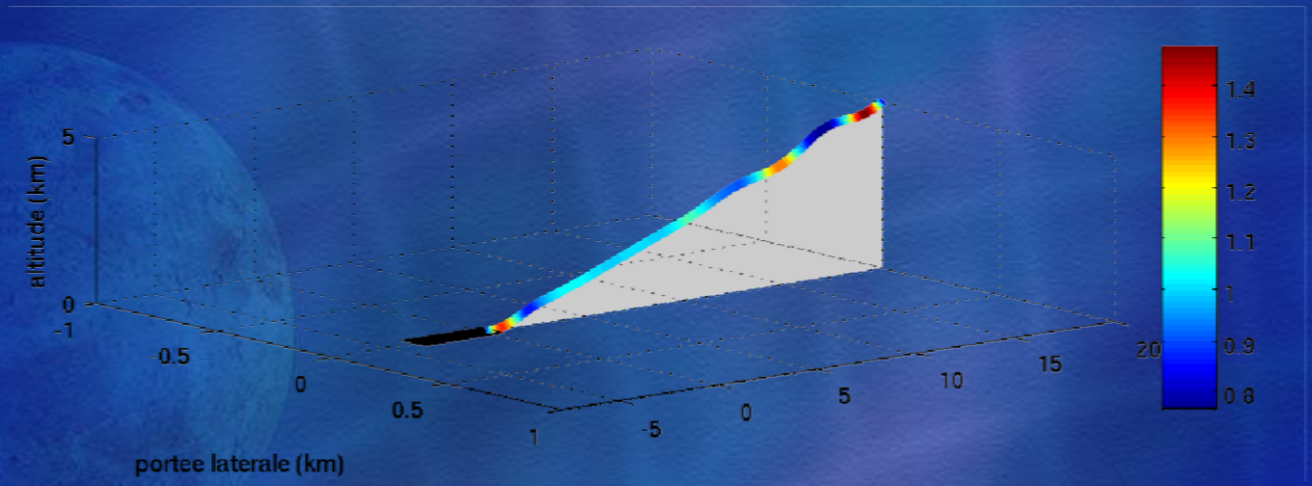

autolanding trajectory profile

Part IV
Fault-tolerant trajectory planning

Main objective:

Design of a fault-tolerant trajectory planner by flatness approach

Motivations:

- flight control law reconfiguration and/or guidance controller adaptation may not be sufficient to recover the vehicle from strong faulty situations,
- aerodynamic forces may change significantly in case of multiple actuators faults

How?

- prediction of surface failure effects at every flight conditions: *trimmability maps*
- *1st solution:* explicit integration of flight quality constraints in the optimal control problem
- *2nd solution:* controlled replanning with exogenous reconfiguration signals (off-line modeling of the trimmability maps)

Trimmability maps:

- Introduced in trajectory planning applications by Air Force Research Lab. (Oppenheimer, 2004)
- Used to obtain the Mach-α regions over which the vehicle can be statically trimmed along the trajectory

Problem (static trimmability problem (Oppenheimer, 2004)). *Let δ be the control surfaces deflection vector associated to rolling, pitching and yawing moments defined respectively by $C_{l_\delta}(\alpha, M, \delta)$, $C_{m_\delta}(\alpha, M, \delta)$ and $C_{n_\delta}(\alpha, M, \delta)$. The pitching moment coefficient in clean configuration is denoted by $C_{m_0}(\alpha, M)$. The* static trimmability problem *is then defined by the feasibility problem*

$$\min_{\delta} J_D = \min_{\delta} \left\| \begin{bmatrix} C_{l_\delta}(\alpha_i, M_j, \delta) \\ C_{m_\delta}(\alpha_i, M_j, \delta) \\ C_{n_\delta}(\alpha_i, M_j, \delta) \end{bmatrix} - \begin{bmatrix} 0 \\ -C_{m_0}(\alpha_i, M_j) \\ 0 \end{bmatrix} \right\|_l$$

s.t.

$$\underline{\delta} \cdot \ \delta \cdot \ \overline{\delta},$$

at each point (α_i, M_j) of the aerodynamic database, where l is a norm.

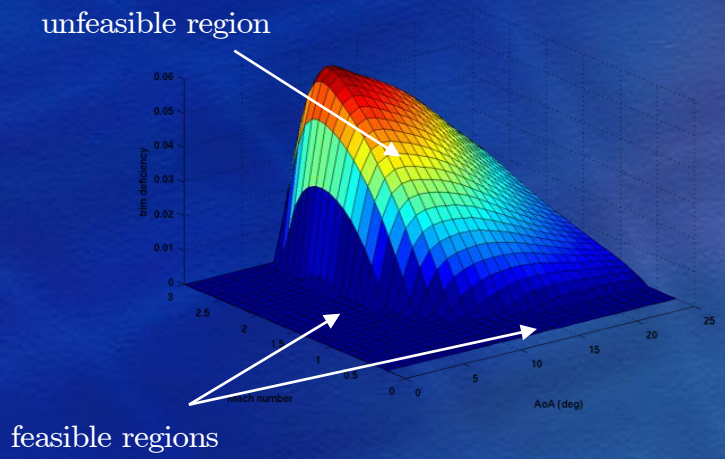

example of 3D trimmability map

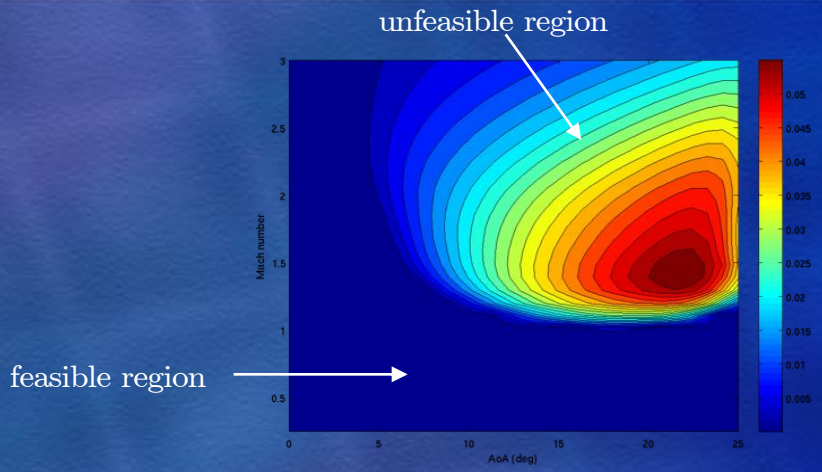

projection in the Mach-α space

- Control surfaces failures effects on the lift and drag coefficients at the point (α_i, M_j) and for $\delta^*_{i,j}$:

$$\begin{cases} C_L(\alpha_i, M_j) = C_{L_0}(\alpha_i, M_j) + C_{L_{\delta^*_{i,j}}}(\alpha_i, M_j, \delta^*_{i,j}), \\ C_D(\alpha_i, M_j) = C_{D_0}(\alpha_i, M_j) + C_{D_{\delta^*_{i,j}}}(\alpha_i, M_j, \delta^*_{i,j}). \end{cases}$$

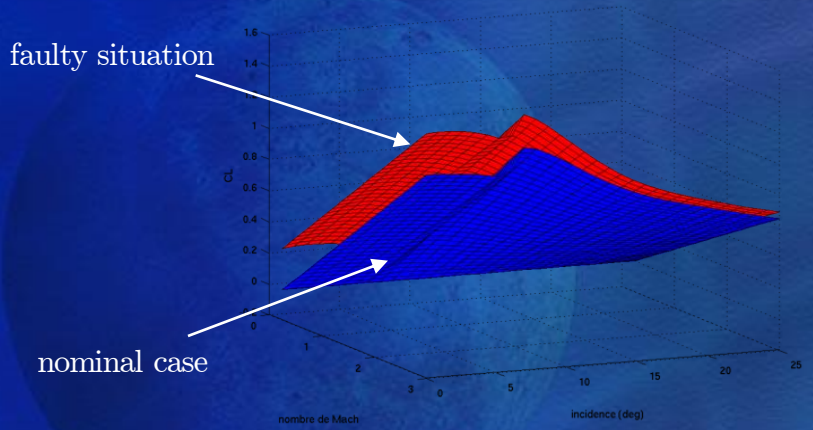

lift coefficient w/wo faults

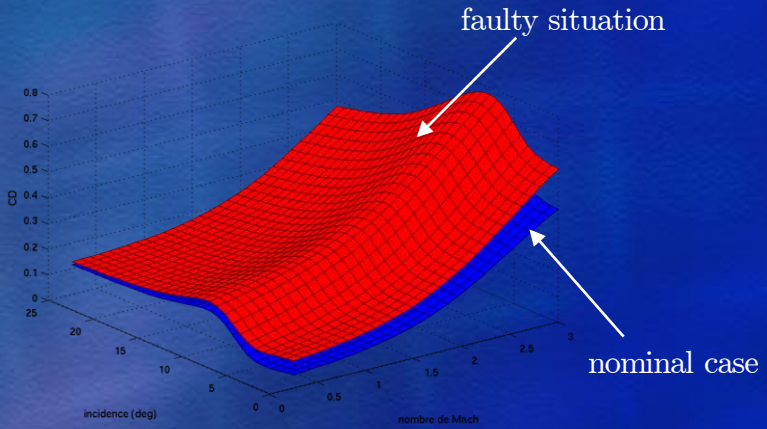

drag coefficient w/wo faults

- 1st solution:

explicit integration of trimmability constraints in the optimal control problem, expressed in the flat output space

$$\min_{\overline{z}(t),\delta(t)} \quad \mathcal{C}_0\left(\psi_x(\overline{z}(t_0)),\psi_u(\overline{z}(t_0),\delta(t_0)),t_0\right) + \int_{t_0}^{t_f} \mathcal{C}_t\left(\psi_x(\overline{z}(t)),\psi_u(\overline{z}(t),\delta(t)),t\right) dt$$
$$+ \mathcal{C}_f\left(\psi_x(\overline{z}(t_f)),\psi_u(\overline{z}(t_f),\delta(t_f)),t_f\right)$$

s.t.

$$\begin{array}{rcccll}
l_0 & \leq & A_0\overline{z}(t_0) & \leq & u_0, & \\
l_t & \leq & A_t\overline{z}(t) & \leq & u_t, & t\in[t_0,t_f],\\
l_f & \leq & A_f\overline{z}(t_f) & \leq & u_f, & \\
L_0 & \leq & c_0\left(\psi_x(\overline{z}(t_0)),\psi_u(\overline{z}(t_0),\delta(t_0))\right) & \leq & U_0, & \\
L_t & \leq & c_t\left(\psi_x(\overline{z}(t)),\psi_u(\overline{z}(t),\delta(t))\right) & \leq & U_t, & t\in[t_0,t_f],\\
L_f & \leq & c_f\left(\psi_x(\overline{z}(t_f)),\psi_u(\overline{z}(t_f),\delta(t_f))\right) & \leq & U_f, &
\end{array}$$

and

$$\underline{\delta} \leq \delta(t) \leq \overline{\delta}, \quad t\in[t_0,t_f].$$

- Advantages: the small number of assumptions about faults types and magnitudes provides a good level of autonomy to the trajectory replanning algorithm.
- Drawbacks: due to the additional number of optimization variables p corresponding to aerodynamic control surfaces, the total number of decision variables of the optimal control problem incrases from $n_{\overline{z}}$ to $n_{\overline{z}}+p$, which directly affects the CPU time.

- 2nd solution:

Off-line computation/modelling of trimmability maps, and online interpolation wrt. the faulty situation

$$
\begin{aligned}
\min_{\overline{z}(t)} \quad & \mathcal{C}_0\left(\psi_x(\overline{z}(t_0)), \psi_u(\overline{z}(t_0), \delta_g), t_0\right) + \int_{t_0}^{t_f} \mathcal{C}_t\left(\psi_x(\overline{z}(t)), \psi_u(\overline{z}(t), \delta_g), t\right) dt \\
& + \mathcal{C}_f\left(\psi_x(\overline{z}(t_f)), \psi_u(\overline{z}(t_f), \delta_g), t_f\right)
\end{aligned}
$$

s.t.

$$
\begin{array}{rcccll}
l_0 & \leq & A_0\overline{z}(t_0) & \leq & u_0, & \\
l_t & \leq & A_t\overline{z}(t) & \leq & u_t, & t \in [t_0, t_f], \\
l_f & \leq & A_f\overline{z}(t_f) & \leq & u_f, & \\
L_0 & \leq & c_0\left(\psi_x(\overline{z}(t_0)), \psi_u(\overline{z}(t_0), \delta_g)\right) & \leq & U_0, & \\
L_t & \leq & c_t\left(\psi_x(\overline{z}(t)), \psi_u(\overline{z}(t), \delta_g)\right) & \leq & U_t, & t \in [t_0, t_f], \\
L_f & \leq & c_f\left(\psi_x(\overline{z}(t_f)), \psi_u(\overline{z}(t_f), \delta_g)\right) & \leq & U_f. &
\end{array}
$$

where $\delta_g \in \Delta \triangleq \{\delta_{g_1}, \delta_{g_2}, \ldots, \delta_{g_K}\}$ is a control surface deflection vector in faulty situation used to drive the optimal control problem.

- Advantages: no additional decision variables enter in the optimal control problem (optimization of flat outputs only): same CPU load as for the initial optimal control problem.
- Drawbacks: the off-line computation and modeling of feasible Mach-α corridors and aerodynamic coefficients in faulty situations requires to predefine a set of representative faulty scenarios, and a great amount of time.

- aerodynamic moment coefficients modeling using analytical neural networks.

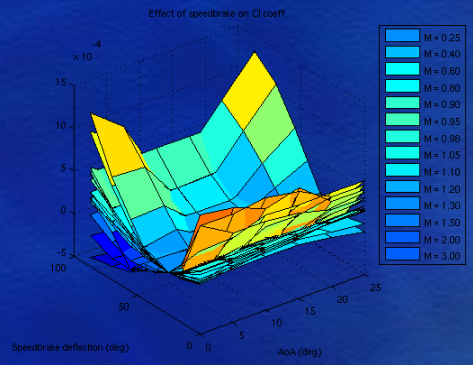

$C_{l_{\delta_{sb}}}$ *coefficient*

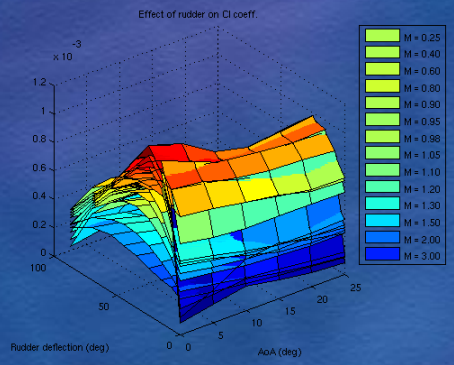

$C_{l_{\delta_r}}$ *coefficient*

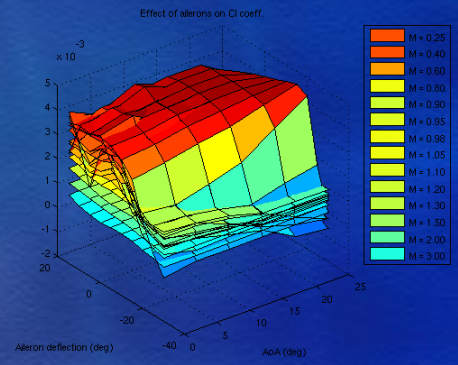

$C_{l_{\delta_a}}$ *coefficient*

- generation of trimmability map for $\delta_{e_{o_l}} = 17^\circ$ and $\delta_{sb} = 0^\circ$ (faulty situation):

$$\min_{\delta} J_D = \min_{\delta} \left\| \begin{bmatrix} T_{(l,n)_{\delta_{i,j}}}(\delta_{i,j}) \\ C_{m_{\delta_{i,j}}}(\alpha_i, M_j, \delta_{i,j}) \end{bmatrix} - \begin{bmatrix} 0 \\ -C_{m0_{i,j}}(\alpha_i, M_j) \end{bmatrix} \right\|_1$$

s.t.

$$\underline{\delta} \leq \delta \leq \overline{\delta},$$

$$T_{(l,n)_{\delta_{i,j}}}(\delta_{i,j}) = \delta_a = \tfrac{1}{4}(\delta_{e_{i_l}} - \delta_{e_{i_r}} + \delta_{e_{o_l}} - \delta_{e_{o_r}}),$$
$$C_{m_{\delta_{i,j}}}(\alpha_i, M_j, \delta_{i,j}) = C_{m_{\delta_e}}(\alpha_i, M_j, \delta_e) + C_{m_{\delta_{bf}}}(\alpha_i, M_j, \delta_{bf}) + C_{m_{\delta_{sb}}}(\alpha_i, M_j, \delta_{sb}),$$
$$\delta = (\delta_{e_{i_l}}, \delta_{e_{i_r}}, \delta_{e_{o_l}}, \delta_{e_{o_r}}, \delta_{bf}, \delta_{sb})^T,$$
$$\overline{\delta} = (\overline{\delta}_{e_{i_l}}, \overline{\delta}_{e_{i_r}}, \overline{\delta}_{e_{o_l}}, \overline{\delta}_{e_{o_r}}, \overline{\delta}_{bf}, \overline{\delta}_{sb})^T,$$
$$\underline{\delta} = (\underline{\delta}_{e_{i_l}}, \underline{\delta}_{e_{i_r}}, \underline{\delta}_{e_{o_l}}, \underline{\delta}_{e_{o_r}}, \underline{\delta}_{bf}, \underline{\delta}_{sb})^T.$$

The fault-tolerant optimal control problem (in the flat output space) is defined by

find $(\overline{z}(t), \lambda, \delta(t))$

s.t.

$$
\begin{array}{ccccccl}
 & & \psi_x(\overline{z}(\tau_0), \lambda) = x_0, & & & & \\
 & & \psi_u(\overline{z}(\tau_0), \lambda, \delta(\tau_0)) = u_0, & & & & \\
 & & \Lambda_\tau(\psi_x(\overline{z}(\tau), \lambda), \psi_u(\overline{z}(\tau), \lambda, \delta(\tau))) = 0, & & & & \tau \in [\tau_0, \tau_f], \\
 & & C_{m_{tot}}(\psi_x(\overline{z}(\tau), \lambda), \psi_u(\overline{z}(\tau), \lambda, \delta(\tau))) = 0, & & & & \tau \in [\tau_0, \tau_f], \\
 & & T_{(l,n)_\delta}(\delta(\tau)) = 0, & & & & \tau \in [\tau_0, \tau_f], \\
0 & \leq & \Gamma\left(\psi_x(\overline{z}(\tau), \lambda), \psi_u(\overline{z}(\tau), \lambda, \delta(\tau))\right) & \leq & \Gamma_{\max}, & & \tau \in [\tau_0, \tau_f], \\
0 & \leq & \overline{q}(\psi_x(\overline{z}(\tau), \lambda)) & \leq & \overline{q}_{\max}, & & \tau \in [\tau_0, \tau_f], \\
u_{\min} & \leq & \psi_u(\overline{z}(\tau), \lambda, \delta(\tau)) & \leq & u_{\max}, & & \tau \in [\tau_0, \tau_f], \\
 & & \psi_x(\overline{z}(\tau_f), \lambda) = x_f, & & & & \\
 & & \psi_u(\overline{z}(\tau_f), \lambda, \delta(\tau_f)) = u_f. & & & &
\end{array}
$$

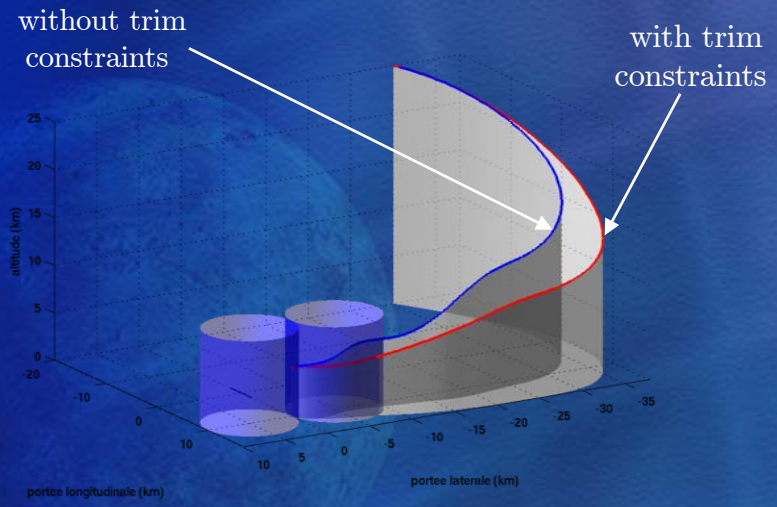

reference trajectory (w/wo trim constraints)

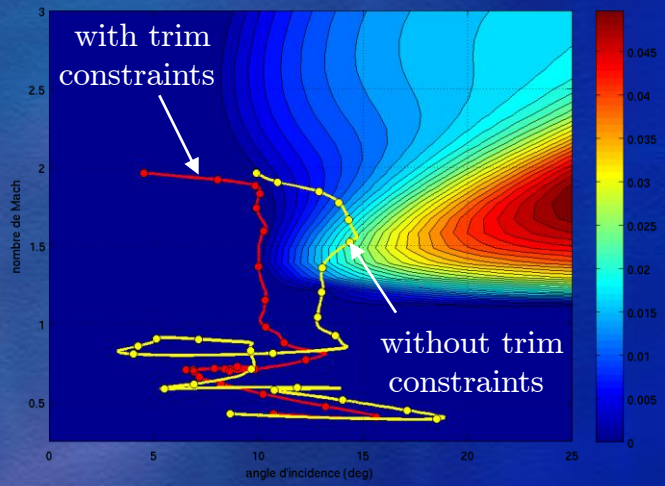

trim map with $\delta_{e_{o_l}} = 17^\circ$ *and* $\delta_{sb} = 0^\circ$

Part V
Integration of aerologic disturbances

Main objective:

Trajectory planning in presence of wind shear disturbances

Motivation:

- strong aerologic disturbances may have adverse effects on guidance and flight control systems

How?

- integration of wind field components in the optimal control problem
- use flatness approach to perform onboard processing

- general wind shear (τ_x, τ_y, τ_h) defined by

$$\begin{cases} \tau_x(x,y,h) = K_{x_1} x^{\sigma_1} y^{\nu_1} h^{\lambda_1} + K_{x_2}, \\ \tau_y(x,y,h) = K_{y_1} x^{\sigma_2} y^{\nu_2} h^{\lambda_2} + K_{y_2}, \\ \tau_h(x,y,h) = K_{h_1} x^{\sigma_3} y^{\nu_3} h^{\lambda_3} + K_{h_2}. \end{cases}$$

$(K_{x_1}, K_{y_1}, K_{h_1})$: wind magnitudes,
$(K_{x_2}, K_{y_2}, K_{h_2})$: constant bias terms,
$(\sigma_i, \nu_i, \lambda_i)$, $i = 1, \ldots, 3$: non-negative powers.

- the new point-mass model is given by

position

$$\begin{cases} x' = \lambda V \cos\chi \cos\gamma + \tau_x(x,y,h), \\ y' = \lambda V \sin\chi \cos\gamma + \tau_y(x,y,h), \\ h' = \lambda V \sin\gamma + \tau_h(x,y,h). \end{cases}$$

velocity

$$\begin{cases} V' = \lambda \left(-\dfrac{D}{m} - g \sin\gamma \right), \\ \gamma' = \lambda \left(\dfrac{L \cos\mu}{mV} - \dfrac{g}{V} \cos\gamma \right), \\ \chi' = \lambda \dfrac{L \sin\mu}{mV \cos\gamma}. \end{cases}$$

- exogenous parameters vector Υ such that

$$\Upsilon = (K_{x_1}, K_{y_1}, K_{h_1}, K_{x_2}, K_{y_2}, K_{h_2}, \sigma_1, \sigma_2, \sigma_3, \nu_1, \nu_2, \nu_3, \lambda_1, \lambda_2, \lambda_3)$$

- integration of the wind field in the OCP expressed in the flat output space

$$
\begin{array}{lll}
\text{find} & (\overline{z}(t), \lambda) & \\
\text{s.t.} & & \\
 & \psi_x(\overline{z}(\tau_0), \lambda, \Upsilon) = x_0, & \\
 & \psi_u(\overline{z}(\tau_0), \lambda, \Upsilon) = u_0, & \\
 & \Lambda_\tau(\psi_x(\overline{z}(\tau), \psi_u(\overline{z}(\tau), \lambda, \Upsilon) = 0, & \tau \in [\tau_0, \tau_f], \\
0 \leq & \Gamma\left(\psi_x(\overline{z}(\tau), \tau), \psi_u(\overline{z}(\tau), \lambda, \Upsilon)\right) & \leq \Gamma_{\max}, \quad \tau \in [\tau_0, \tau_f], \\
0 \leq & \overline{q}(\psi_x(\overline{z}(\tau), \lambda, \Upsilon) & \leq \overline{q}_{\max}, \quad \tau \in [\tau_0, \tau_f], \\
u_{\min} \leq & \psi_u(\overline{z}(\tau), \lambda, \Upsilon) & \leq u_{\max}, \quad \tau \in [\tau_0, \tau_f], \\
 & \psi_x(\overline{z}(\tau_f), \lambda, \Upsilon) = x_f, & \\
 & \psi_u(\overline{z}(\tau_f), \lambda, \Upsilon) = u_f. &
\end{array}
$$

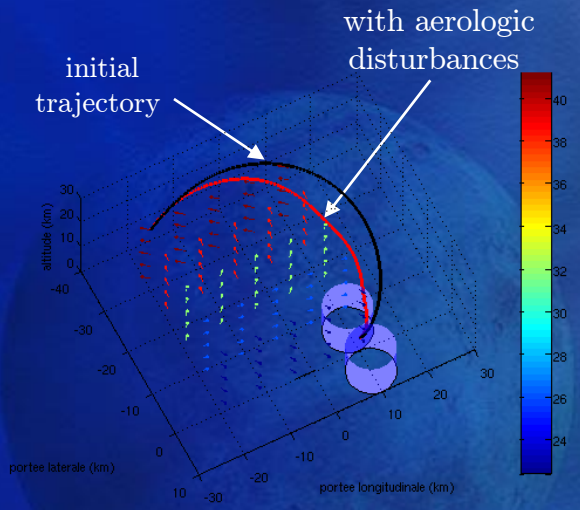

3D reference trajectories

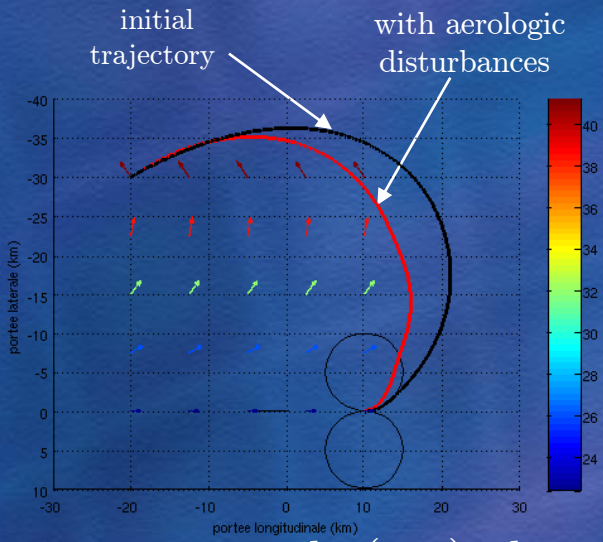

projection in the (x, y) plane

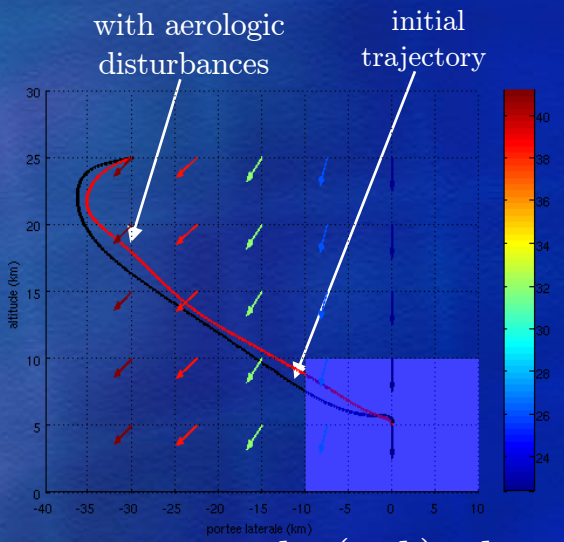

projection in the (x, h) plane

Part VI
Optimal control problem convexification

Main objective:

Convexification of the optimal control problem by deformable shapes.

Motivations:

- the OCP described in the flat output space is often highly nonlinear and nonconvex (Ross, 2006)
- to guarantee global convergence of NLP solvers

How?

- the convexification problem is solved by a genetic algorithm in order to get a global solution
- development of a Matlab software library (by the author): OCEANS (Optimal Convexification by Evolutionary Algorithm aNd Superquadrics)

Superquadric shapes

Superquadrics:

- generalization in 3 dimensions of the superellipses (Barr, 1981)
- used to perform a trade-off between the complexity of the shapes and the numerical tractability in high order flat output spaces

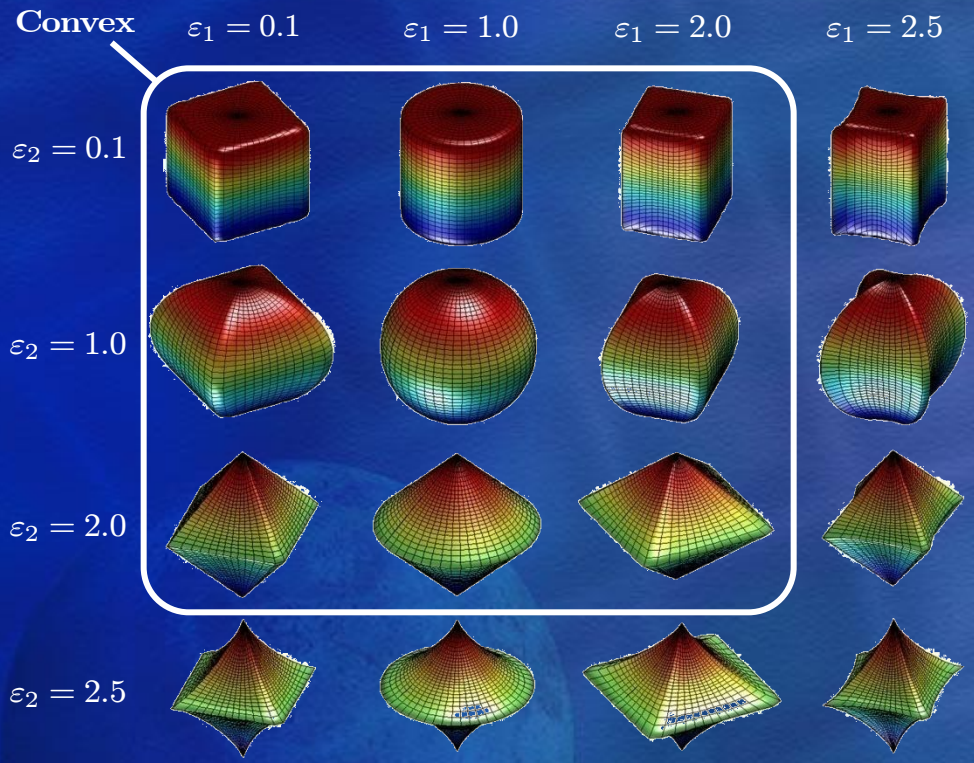

examples of 3D superquadrics

Advantages:

- compactness of the representation
- an explicit parametrization exists

Drawbacks:

- limited number of shapes
- symetric shapes only

Necessity to obtain new mathematical results about n-D superquadrics and to introduce additional convexity-preserving geometric transformations

Introduction of n-D transformations: rotation, translation and linear pinching (defined in the PhD dissertation)

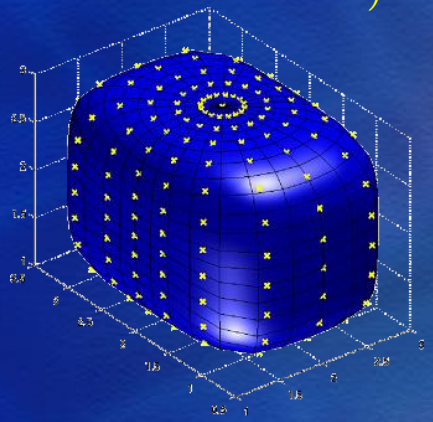

initial 3D superquadric

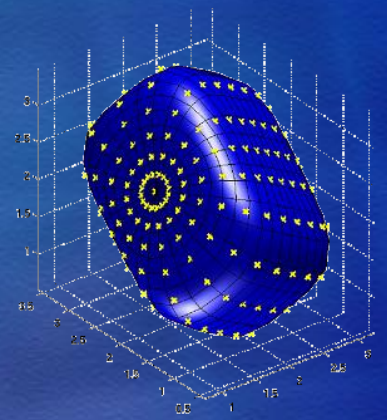

effect of a 3D rotation

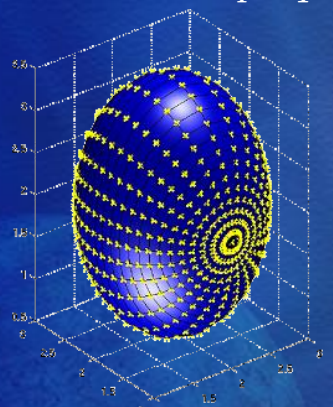

initial 3D superquadric

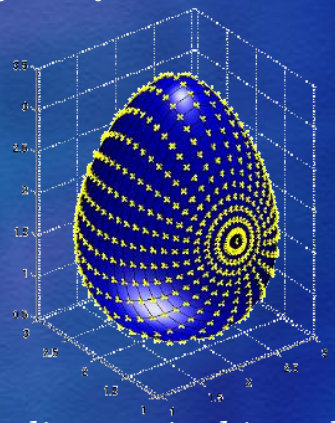

effect of a linear pinching along z axis

The set Ψ contains the sizing parameters needed to obtain a positioned, oriented and bended superquadric shape

$$\Psi = \{ \underbrace{a_1, \ldots, a_n}_{\text{semi-major axes}} , \underbrace{\varepsilon_1, \ldots, \varepsilon_{n-1}}_{\text{roundness par.}} , \underbrace{\Phi_1, \ldots, \Phi_{n(n+1)/2}}_{\text{rotation par.}} , \underbrace{d_1, \ldots, d_n}_{\text{translation par.}} , \underbrace{v_1, \ldots, v_{n-1}}_{\text{pinching par.}} \}$$

Proposition (trigonometric parametrization of a bended n-D superellipsoid (**Morio,2008**)). *Let $\mathcal{S}$ a superquadric ellipsoid of size n, described by the vector Ψ. Then, the corresponding* trigonometric parametrization, *with cartesian coordinates x_i, $i = 1, \ldots, n$, is defined by*

$$x_i = \begin{cases} a_1(v_1 \sin^{\varepsilon_p - 1}\theta_{p-1} \prod_{j=p}^{n-1} \cos^{\varepsilon_j}\theta_j + 1) \prod_{k=1}^{n-1} \cos^{\varepsilon_k}\theta_k, & i = 1, \\ a_i(v_i \sin^{\varepsilon_p - 1}\theta_{p-1} \prod_{j=p}^{n-1} \cos^{\varepsilon_j}\theta_j + 1) \sin^{\varepsilon_{i-1}}\theta_{i-1} \prod_{k=i}^{n-1} \cos^{\varepsilon_k}\theta_k, & i = 2, \ldots, n-1, \quad i \neq p, \\ a_p \sin^{\varepsilon_p - 1}\theta_{p-1} \prod_{j=p}^{n-1} \cos^{\varepsilon_j}\theta_j, & i = p, \\ a_n(v_n \sin^{\varepsilon_p - 1}\theta_{p-1} \prod_{j=p}^{n-1} \cos^{\varepsilon_j}\theta_j + 1) \sin^{\varepsilon_{n-1}}\theta_{n-1}, & i = n, \end{cases}$$

where p is the pinching direction ($v_p = 0$). In addition, the vector of anomalies θ satisfies $\theta_i \in [-\pi, \pi[$ if $i = 1$ and $\theta_i \in [-\frac{\pi}{2}, \frac{\pi}{2}]$ if $i = 2, \ldots, n-1$.

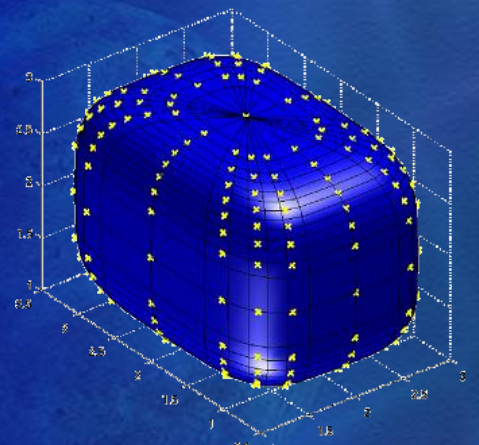

3D trigonometric parametrization

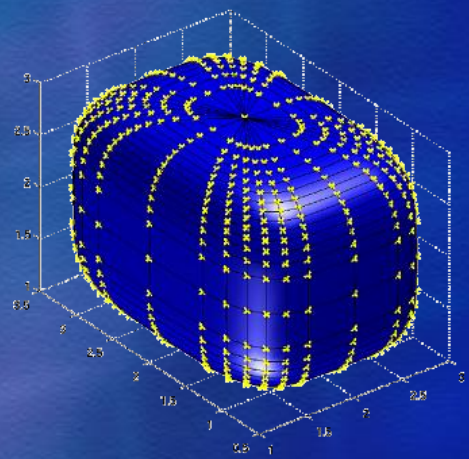

variation of the number of anomalies

Proposition (angle-center parametrization of a bended n-D superellipsoid (**Morio,2008**)). *Let $\mathcal{S}$ be a superquadric ellipsoid of size n, described by the vector Ψ. Then, the corresponding* angle-center parametrization, *with cartesian coordinates x_i, $i = 1, \ldots, n$, is defined by*

$$x_i = \begin{cases} r(\theta)\left(\dfrac{v_1}{a_p} r(\theta) \sin\theta_{p-1} \displaystyle\prod_{j=p}^{n-1} \cos\theta_j + 1\right) \displaystyle\prod_{k=1}^{n-1} \cos\theta_k, & i = 1, \\ r(\theta)\left(\dfrac{v_i}{a_p} r(\theta) \sin\theta_{p-1} \displaystyle\prod_{j=p}^{n-1} \cos\theta_j + 1\right) \sin\theta_{i-1} \displaystyle\prod_{k=i}^{n-1} \cos\theta_k, & i = 2, \ldots, n-1, i \neq p, \\ r(\theta) \sin\theta_{p-1} \displaystyle\prod_{j=p}^{n-1} \cos\theta_j, & i = p, \\ r(\theta)\left(\dfrac{v_n}{a_p} r(\theta) \sin\theta_{p-1} \displaystyle\prod_{j=p}^{n-1} \cos\theta_j + 1\right) \sin\theta_{n-1}, & i = n, \end{cases}$$

where p is the pinching direction ($v_p = 0$). The radius $r(\theta) = \frac{1}{\chi_{n,n}}$ is given by

$$\begin{cases} \chi_{n,2} = \left[\left(\dfrac{\prod_{k=1}^{n-1} \cos\theta_k}{a_1}\right)^{\frac{2}{\varepsilon_1}} + \left(\dfrac{\sin\theta_1 \prod_{k=2}^{n-1} \cos\theta_k}{a_2}\right)^{\frac{2}{\varepsilon_1}}\right]^{\frac{\varepsilon_1}{2}}, & j = 2, \\ \chi_{n,j} = \left[\left(\chi_{n,j-1}\right)^{\frac{2}{\varepsilon_{j-1}}} + \left(\dfrac{\sin\theta_{j-1} \prod_{k=j}^{n-1} \cos\theta_k}{a_j}\right)^{\frac{2}{\varepsilon_{j-1}}}\right]^{\frac{\varepsilon_{j-1}}{2}}, & j = 3, \ldots, n, \end{cases}$$

with $\theta_i \in [-\pi, \pi[$ if $i = 1$ and $\theta_i \in [-\frac{\pi}{2}, \frac{\pi}{2}]$ if $i = 2, \ldots, n-1$.

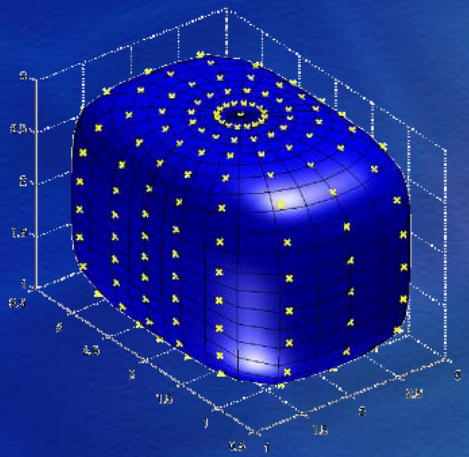

No. of anomalies

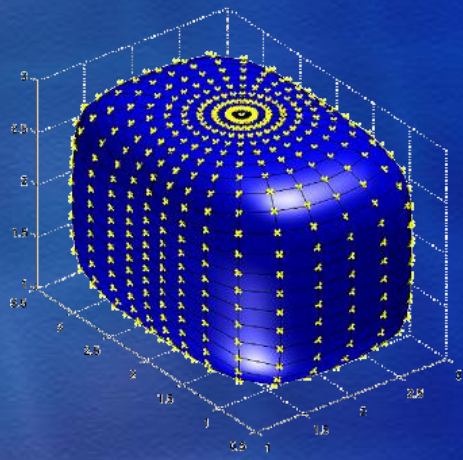

3D angle-center parametrization

variation of the number of anomalies

The angle-center parametrization results in a better sampling of the superquadric surface for smooth convex shapes

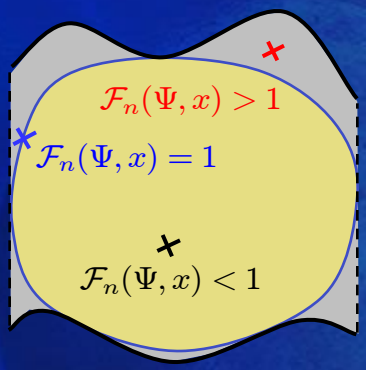

Proposition (inside-outside function of a bended n-D superellipsoid (**Morio,2008**)). *Let $\mathcal{S}$ be a superellipsoid of size n, described by the vector Ψ. Then, the corresponding (implicit)* inside-outside function $\mathcal{F}_n(\Psi,x)=\Lambda_{n,n}(\Psi,x)$, *is defined by the recursive expression*

$$\begin{cases} \Lambda_{n,2}(\Psi,x)=\left(\dfrac{x_1}{a_1\left(\frac{v_1}{a_p}x_p+1\right)}\right)^{\frac{2}{\varepsilon_1}}+\left(\dfrac{x_2}{a_2\left(\frac{v_2}{a_p}x_p+1\right)}\right)^{\frac{2}{\varepsilon_1}}, \\ \Lambda_{n,k}(\Psi,x)=\left(\Lambda_{n,k-1}(\Psi,x)\right)^{\frac{\varepsilon_{k-2}}{\varepsilon_{k-1}}}+\left(\dfrac{x_k}{a_k\left(\frac{v_k}{a_p}x_p+1\right)}\right)^{\frac{2}{\varepsilon_{k-1}}}, \end{cases}$$

where $v_p=0$ in the pinching direction p.

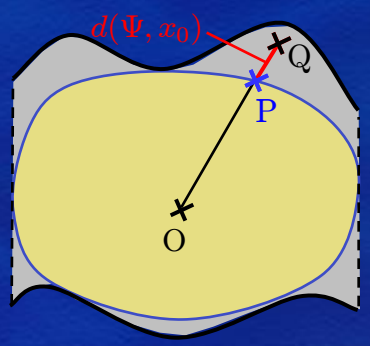

Proposition (n-D euclidean radial distance (**Morio,2008**)). *The* euclidean radial distance $d(\Psi, x_0)$ *is defined as being the distance between a point* Q *with coordinates* x_0*, and a point* P *with coordinates* x_s*, corresponding to the projection of* Q *onto the superellipsoid, along the direction defined by the point* Q *and the center of the geometric shape. For an arbitrary* n*-D superellipsoid, described by the vector* Ψ*, the expression of the radial euclidean distance* $d(\Psi, x_0) = |x_0 - x_s|$ *is given by*

$$d(\Psi, x_0) = |x_0| \cdot \left| 1 - (\mathcal{F}_n(\Psi, x_0))^{-\frac{\varepsilon_{n-1}}{2}} \right|,$$

Proposition (volume of a bended n-D superellipsoid (**Morio,2008**)). *Let* $\mathcal{S}$ *be a bended superellipsoid of size* n*, described by the vector* Ψ*. The volume* $V_n(\Psi)$ *of* $\mathcal{S}$ *is defined by*

$$V_n(\Psi) = 2a_n \left[\prod_{\substack{i=1 \\ i \neq p-1}}^{n-1} a_i \varepsilon_i B\left(\frac{\varepsilon_i}{2}, i\frac{\varepsilon_i}{2} + 1\right) \right] \cdot \left[a_{p-1}\varepsilon_{p-1} \sum_{|\alpha|=0}^{n-1} v^\alpha B\left(\frac{|\alpha|+1}{2}\varepsilon_{p-1}, \frac{p-1}{2}\varepsilon_{p-1} + 1\right) \right],$$

where the multi-index $\alpha = (\alpha_1, \ldots, \alpha_{p-1}, 0, \alpha_{p+1}, \ldots, \alpha_n)$ *satisfies*

$$v^\alpha = \prod_{k=1}^{n} v_k^{\alpha_k}, \quad |\alpha| = \sum_{j=1}^{n} \alpha_j, \quad \alpha_i \in \{0, 1\}, \quad i = 1, \ldots, n,$$

In addition, the Beta function $B(x, y)$ *is linked to the Gamma function by*

$$B(x, y) = 2\int_0^{\pi/2} \sin^{2x-1}\phi \cos^{2y-1}\phi d\phi = \frac{\Gamma(x)\Gamma(y)}{\Gamma(x+y)},$$

the Gamma being typically defined by

$$\Gamma(x) = \int_0^\infty \exp^{-t} t^{x-1} dt,$$

Superellipsoidal annexion problem

We assume that the nonconvex domain may be described by means of one or more analytical expressions defined by

$$f_{min} \leq f_{nc}(x) \leq f_{max},$$

where x is a set of variables of size n.

Problem (superellipsoidal annexion problem (**Morio,2008**)). *Let $\mathcal{S}$ be a superellipsoid of size n, described by the vector Ψ. The* superellipsoidal annexion problem *(or convexification problem) consists then in finding the optimal parameters Ψ^* associated to the biggest superellipsoid $\mathcal{S}_{opt}$ contained inside the feasible domain (supposed to be nonconvex) defined by the analytical expression f_{nc}, such that*

$$\max_{\Psi} \quad \widetilde{V}_n(\Psi)$$

$$s.t. \quad \begin{cases} \mathcal{F}_n(\Psi, x) \leq 1, \\ f_{min} \leq f_{nc}(x) \leq f_{max}, \\ x_i^l \leq x_i \leq x_i^u, \quad i = 1, \ldots, n. \end{cases}$$

where the normalized superquadric volume $\widetilde{V}_n(\Psi)$ is defined by $\widetilde{V}_n(\Psi) = V_n(\Psi)^{\frac{1}{n}}$, and $\mathcal{F}_n(\Psi, x)$ is the inside-outside function.The variables x are the cartesian coordinates associated to a predefined number of sampling points at the supersuadric surface.

Resolution of the convexification problem

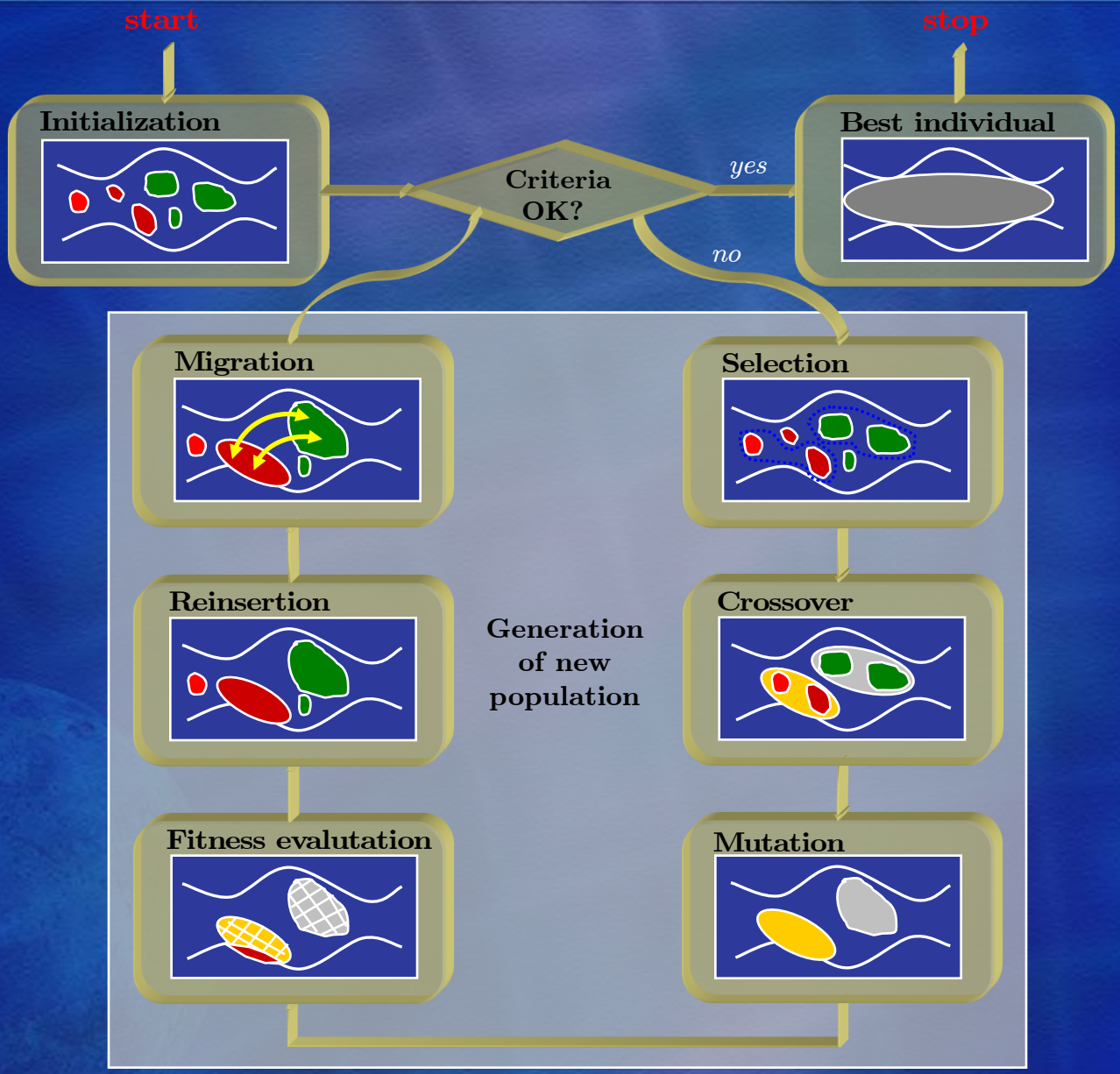

Multi-population extended genetic algorithm adapted to the problem at hand

- the *convex* optimal control problem in the flat output space is given by

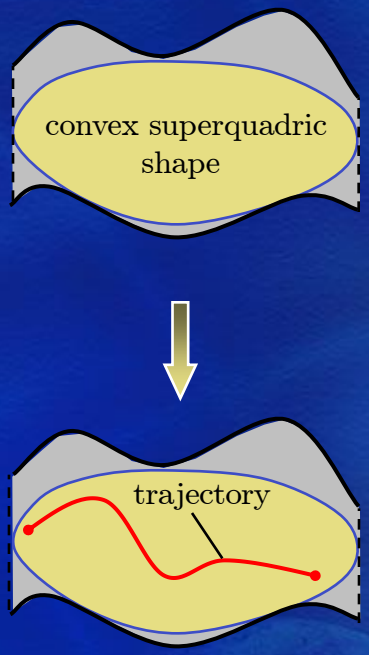

$$
\begin{aligned}
\min_{\overline{z}(t)} \quad & \mathcal{C}_0\left(\psi_x(\overline{z}(t_0)), \psi_u(\overline{z}(t_0)), t_0\right) + \int_{t_0}^{t_f} \mathcal{C}_t\left(\psi_x(\overline{z}(t)), \psi_u(\overline{z}(t)), t\right) dt \\
& + \mathcal{C}_f\left(\psi_x(\overline{z}(t_f)), \psi_u(\overline{z}(t_f)), t_f\right)
\end{aligned}
$$

s.t.

$$
\begin{array}{ccccc}
l_0 & \leq & A_0\overline{z}(t_0) & \leq & u_0, \\
l_t & \leq & A_t\overline{z}(t) & \leq & u_t, \quad t \in [t_0, t_f], \\
l_f & \leq & A_f\overline{z}(t_f) & \leq & u_f, \\
L_0 & \leq & c_0\left(\psi_x(\overline{z}(t_0)), \psi_u(\overline{z}(t_0))\right) & \leq & U_0, \\
0 & \leq & \mathcal{F}_n^i\left(\Psi^*, \overline{z}(t)\right) & \leq & 1, \quad t \in [t_0, t_f], \\
L_f & \leq & c_f\left(\psi_x(\overline{z}(t_f)), \psi_u(\overline{z}(t_f))\right) & \leq & U_f.
\end{array}
$$

where $\mathcal{F}_n^i\left(\Psi^*, \overline{z}(t)\right)$, $i = 1, \ldots, n_s$, are the inside-outside functions associated to the optimized convex shapes.

- boundary constraints must be met: $\mathcal{F}_n\left(\Psi^*, \overline{z}(t_0)\right) \cdot \ 1$ and $\mathcal{F}_n\left(\Psi^*, \overline{z}(t_f)\right) \cdot \ 1$. It is possible to check if the extremal points of the trajectory are lying inside the convex envelopes by computing the associated n-D radial euclidean distances
- a convex cost functional may be obtained by using the same process.

Some simple examples in 3 dimensions

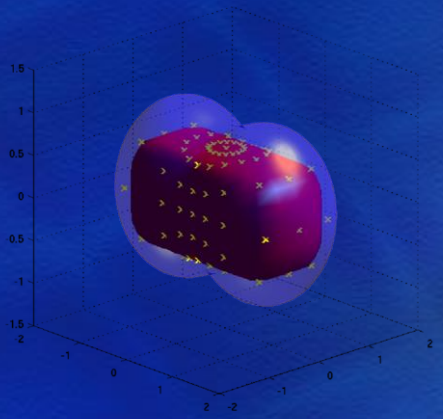

(a)

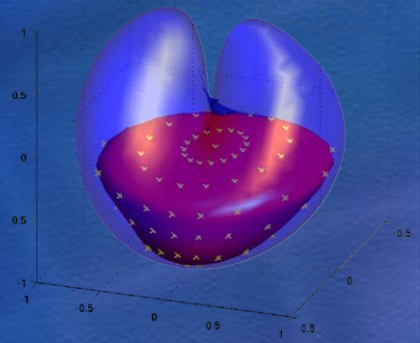

(b)

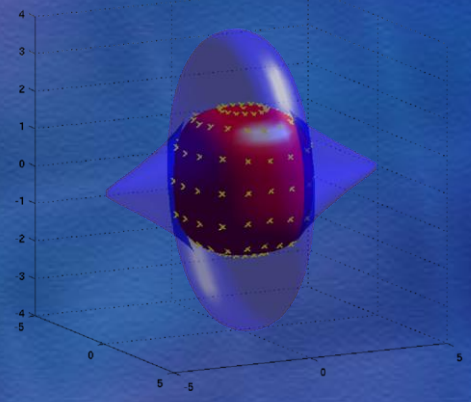

(c)

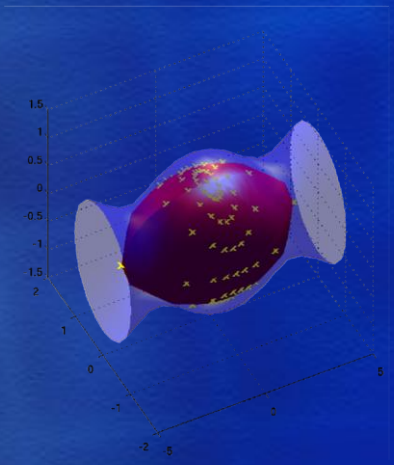

(d)

The initial nonconvex domains are defined by

(a) $D_1 = \{x | x \in \mathbb{R}^3, \left((x_1 - 0.9)^2 + x_2^2 + x_3^2 - 1\right)\left((x_1 + 0.9)^2 + x_2^2 + x_3^2 - 1\right) - 0.3 \cdot \ 0\}$,

(b) $D_2 = \{x | x \in \mathbb{R}^3, 4x_1^2\left(x_1^2 + x_2^2 + x_3^2 + x_3\right) + x_2^2\left(x_2^2 + x_3^2 - 1\right) \cdot \ 0\}$,

(c) $D_3 = \{x | x \in \mathbb{R}^3, \left(\sqrt{x_1^2 + x_3^2} - 3\right)^3 + x_2^2 - 1 \cdot \ 0\}$,

(d) $D_4 = \{x | x \in \mathbb{R}^3, x_2^2 + x_3^2 - 0.5\cos x_1 \cos x_2 - 1 \cdot \ 0\}$.

- example: dynamic pressure constraint along the TAEM trajectory, expressed wrt. flat outputs

$$0 \leq \frac{1}{2}\rho_0 \exp\left(-\frac{z_3}{H_0}\right) S \frac{\sqrt{z1'^2 + z2'^2 + z3'^2}}{\lambda} \leq \overline{q}_{\max}.$$

- nonconvex constraint: exponentially decreasing spherical shape
- Inner approximation by a 5-D superellipsoid described by

$$\Psi = \{ \underbrace{a_1, \ldots, a_5}_{\text{semi-major axes}} , \underbrace{\varepsilon_1, \ldots, \varepsilon_4}_{\text{roundness par.}} , \underbrace{\Phi_1, \ldots, \Phi_{15}}_{\text{rotation par.}} , \underbrace{d_1, \ldots, d_5}_{\text{translation par.}} , \underbrace{v_1, \ldots, v_4}_{\text{pinching par.}} \}.$$

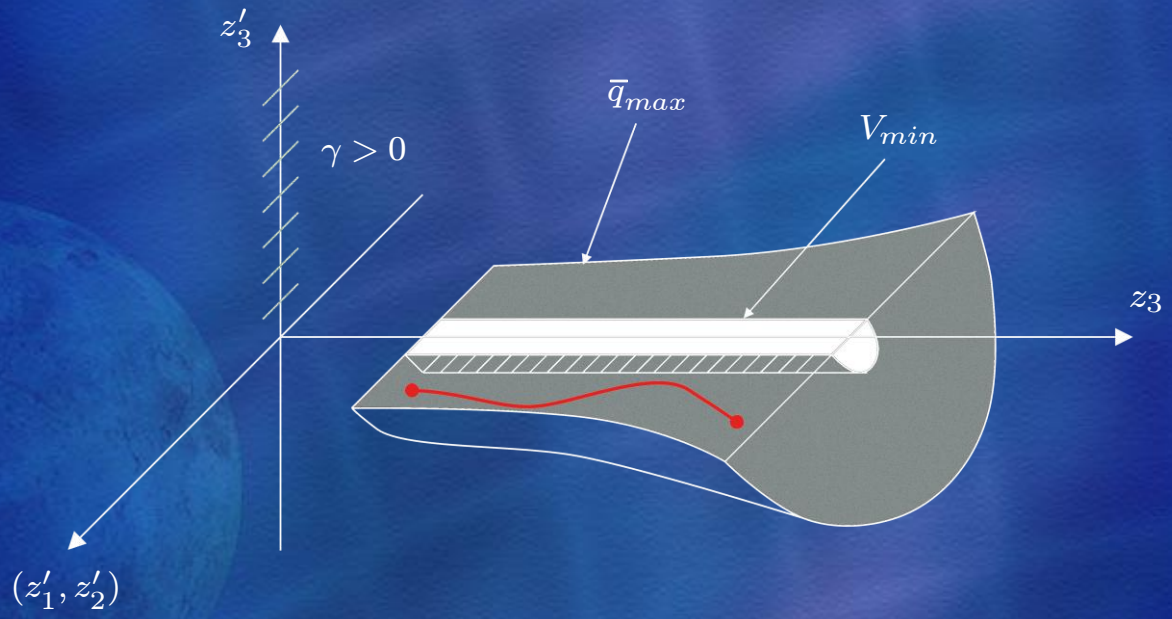

geometric interpretation

Convexification of the optimal control problem

- simple genetic algorithm tuning parameters provide good results
- the inside-outside function $\mathcal{F}_{\overline{q}}(\Psi^*, \overline{z})$ is given by

$$\mathcal{F}_{\overline{q}}(\Psi^*, \overline{z}) = \left[\left(0.8.10^{-4} z_3 - 1.2\right)^{20} + \left(\frac{z_1'}{3.2.10^4 + 5.3 z_3} \right)^{20} \right]^{0.1} + \left(\frac{z_2'}{3.5.10^4 + 5.9 z_3} \right)^2 + \left(\frac{z_3'}{3.1.10^4 + 5.3 z_3} \right)^2 + . \left(\frac{\lambda}{45.7 + 0.76.10^{-2} z_3} \right)^2,$$

where Ψ^* are optimal defining parameters and $\overline{z} = (z_3, z_1', z_2', z_3', \lambda)$.

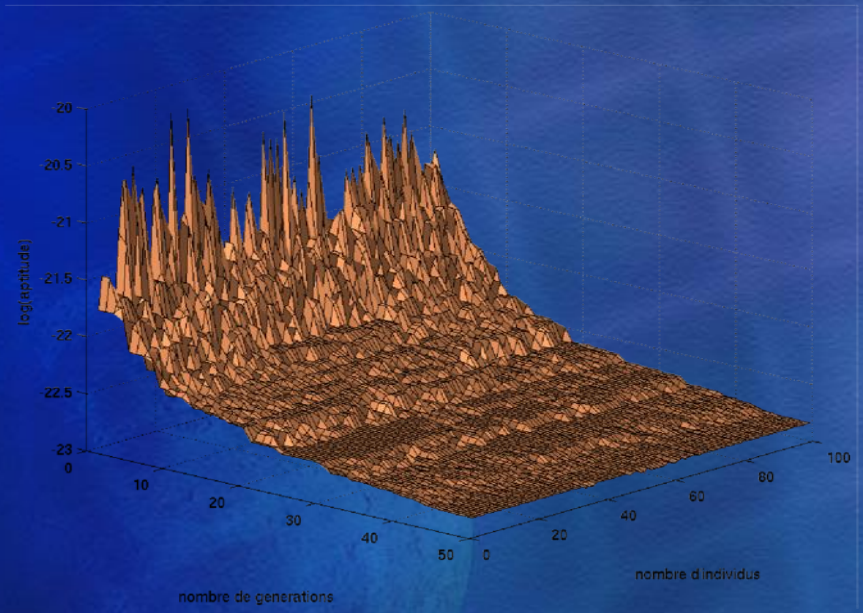

individuals fitnesses wrt. generations

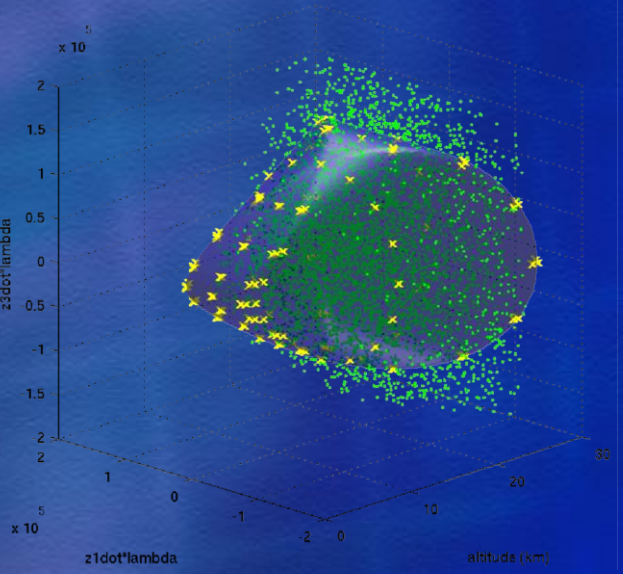

approximating convex shape

- other nonconvex trajectory constraints convexified by using the same process

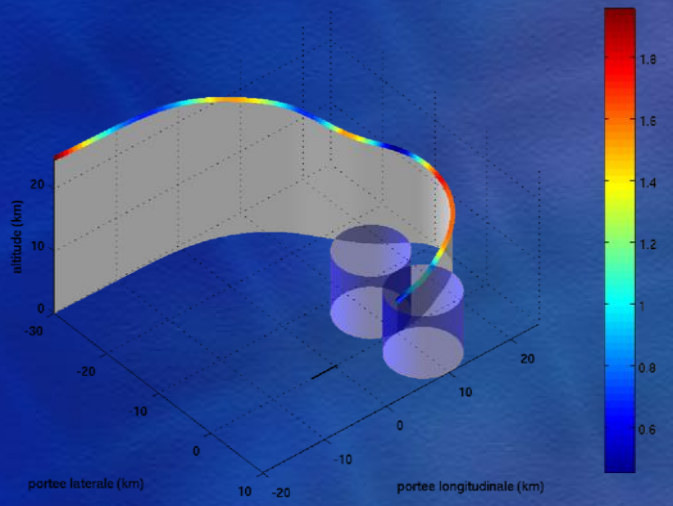

3D reference trajectory

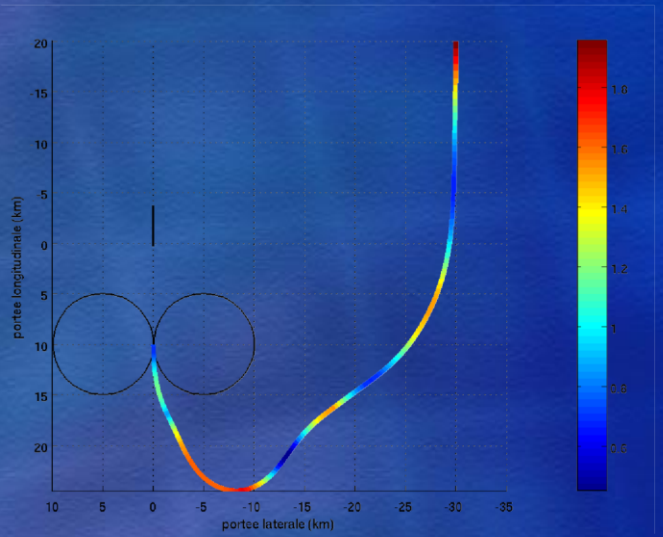

projection in the horizontal plane

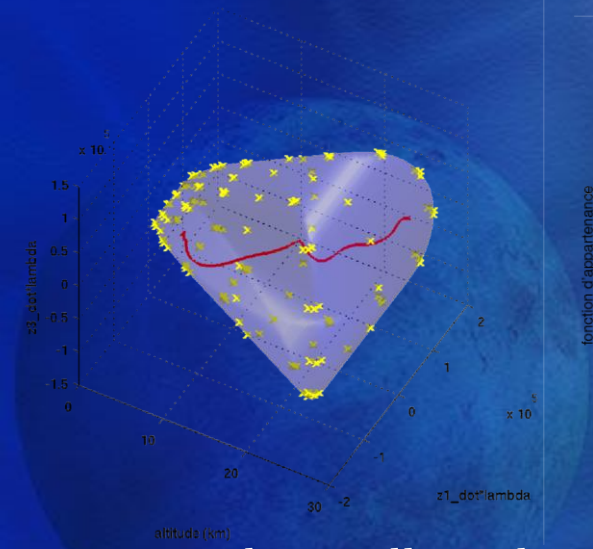

optimized superellipsoid

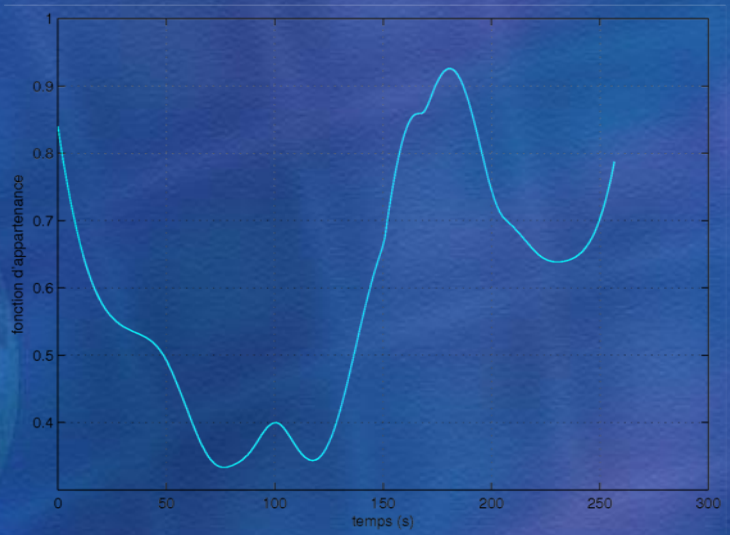

superellipsoid inside-outside function

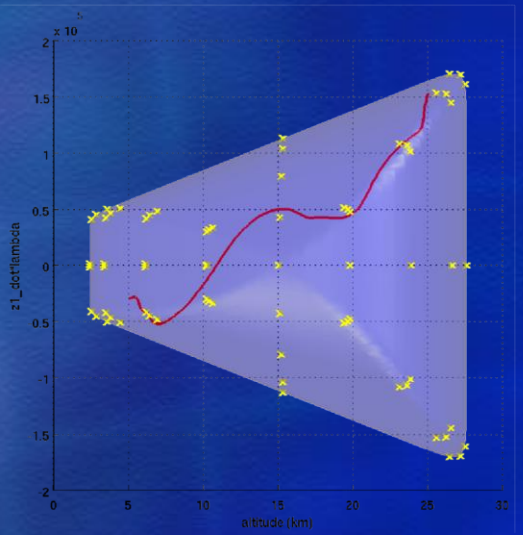

optimized superellipsoid

Conclusions ...

Research work includes contributions in 3 directions:

- Theoretical: necessary and sufficient conditions of δ-flatness for linear delay systems (not presented)
- Methodological: design of an autonomous guidance law
  - modelling, problem formulation and onboard solving using flatness theory
  - convexification by superquadric shapes
  - fault-tolerant trajectory planning by integration of trimmability constraints
  - integration of aerologic disturbances
- Application to an atmospheric reentry mission:
  - Terminal Area Energy Management (TAEM) and Auto-Landing (A&L) phases of Shutle orbiter STS-1 vehicle

... and perspectives

- Application of the autonomous guidance law to other space missions: unmanned aerial vehicles, satellite orbital maneuvers, autonomous missile guidance, ...
- Onboard generation of fully constrained 6 dof trajectories (integration of flight control equations): may be used to bound the guidance inputs rates $(\dot{\alpha}, \dot{\beta}, \dot{\mu})$ in presence of a faulty situation
- Adequately manage the transcient regime between the occurence of a fault and the integration of the reshaped trajectory in the GNC system
- Transform the convex optimal control problem into a semi-definite programming problem: requires to describe superquadric shapes as linear matrix inequalities

International journal papers

[1] V. Morio, F. Cazaurang and P. Vernis, "Flatness-based Hypersonic Reentry Guidance of a Lifting-body Vehicle," **Control Engineering Practice**, 17(5):588-596, May 2009.

[2] V. Morio, F. Cazaurang, A. Zolghadri and P. Vernis, "Onboard Path Planning for Reusable Launch Vehicles. Application to the Shuttle Orbiter Reentry Mission," **International Review of Aerospace Engineering**, 1(6), December 2008.

[3] F. Cazaurang, V. Morio, A. Falcoz, D. Henry and A. Zolghadri, "New Model-Based Strategies for Guidance and Health Monitoring of Experimental Reentry Vehicles," **International Review of Aerospace Engineering**, 1(5):458-463, October 2008.

[4] V. Morio, F. Cazaurang, A. Falcoz and P. Vernis, "Robust Terminal Area Energy Management Guidance using Flatness Approach," **IET Control Theory and Applications**, 2009.

[5] V. Morio, F. Cazaurang, A. Zolghadri and J. Lévine, "A Computation of δ-Flat Outputs for Linear Delay and Infinite Dimensional Systems," **IEEE Transactions in Automatic Control**, *in preparation*.

Conference papers

[1] V. Morio, F. Cazaurang and A. Zolghadri and P. Vernis, "A new Path Planner based on Flatness Approach. Application to an Atmospheric Reentry Mission," **Proceedings of the European Control Conference (ECC'09)**, Budapest, Hungary. 2009.

[2] V. Morio, F. Cazaurang and A. Zolghadri, "On the Formal Characterization of Reduced-Order Flat Outputs over an Ore Algebra," **Proceedings of the 2nd IEEE Multiconference on Systems and Control (MSC) / 9th IEEE International Symposium on Computer-aided Control System Design (CACSD)**, pp. 207-214, San Antonio, Texas. 2008.

Conference papers (cont'd)

[3] V. Morio, F. Cazaurang and A. Zolghadri, "An Effective Algorithm for Analytical Computation of Flat Outputs over the Weyl Algebra," **Proceedings of the 17th IFAC World Congress**, Seoul, Korea. 2008.

[4] V. Morio, F. Cazaurang and A. Zolghadri, "Sur la Caractérisation Formelle de Sorties Plates d'Ordre Réduit sur un Algèbre de Weyl," **Actes de la Conférence Internationale Francophone d'Automatique**, Bucarest, Roumanie. 2008.

[5] V. Morio, F. Cazaurang, A. Zolghadri and P. Vernis, "Onboard Terminal Area Management Path Planning using Flatness Approach. Application to Shuttle orbiter STS-1 Vehicle," **Proceedings of the 2nd International ARA Days**, Arcachon, France. 2008.

[6] V. Morio, A. Falcoz, F. Cazaurang, D. Henry, A. Zolghadri, M. Ganet, P. Vernis and E. Bornschlegl, "SICVER Project: Innovative FDIR Strategies for Experimental Reentry Vehicles," **Proceedings of the 2nd International ARA Days**, Arcachon, France. 2008.

[7] V. Morio, A. Falcoz, P. Vernis and F. Cazaurang, "On the design of a flatness-based guidance algorithm for the terminal area energy management of a winged-body vehicle," **Proceedings of the 17th IFAC Symposium on Automatic Control in Aerospace**, Toulouse, France. 2007.

[8] P. Vernis, V. Morio and E. Ferreira, "Genetic Algorithm for coupled RLV trajectory and guidance optimization," **Proceedings of the 17th IFAC Symposium on Automatic Control in Aerospace**, Toulouse, France. 2007.

[9] V. Morio, P. Vernis and F. Cazaurang, "Hypersonic Reentry and Flatness Theory. Application to medium L/D Entry Vehicle," **Proceedings of the 1st International ARA Days**, Arcachon, France. 2006.

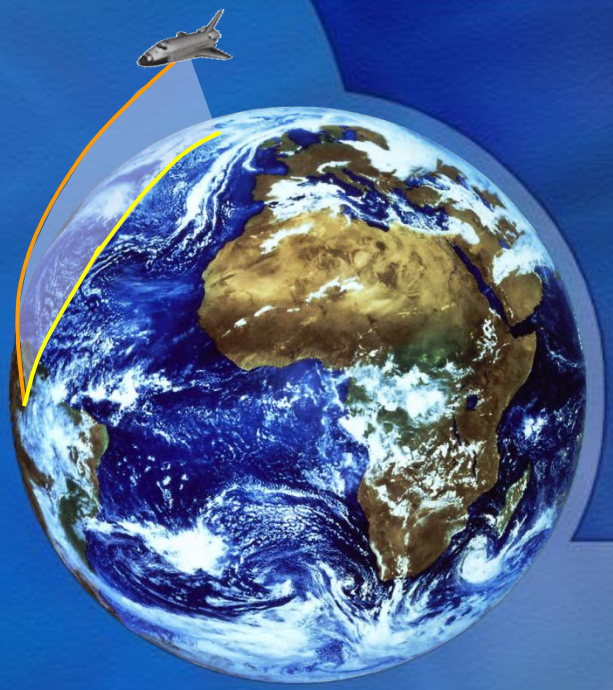

THANK YOU FOR

YOUR ATTENTION